FINAL REPORT

Contract No. NAS8-25055
CR-123830

STUDY OF DENSE ALUMINUM PLASMAS

by

F. C. Todd

Submitted to

National Aeronautics and Space Administration
George C. Marshall Space Flight Center
Marshall Space Flight Center, Alabama

Submitted by

The University of Alabama in Huntsville
Division of Graduate Programs and Research
Research Institute
P. O. Box 1247
Huntsville, Alabama 35807

FINAL REPORT

Contract No. NAS8-25055

STUDY OF DENSE ALUMINUM PLASMAS

by

F. C. Todd

Submitted to

National Aeronautics and Space Administration
George C. Marshall Space Flight Center
Marshall Space Flight Center, Alabama

Submitted by

The University of Alabama in Huntsville
Division of Graduate Programs and Research
Research Institute
P. O. Box 1247
Huntsville, Alabama 35807

TABLE OF CONTENTS

	Page
STATUS OF STUDIES ON BUMPER PLATE PENETRATION AND SUBSEQUENT PHENOMENA	1
SURVEY OF SCOPE OF THE PROJECTS	1
PHASE ONE	5
ABLATION OF SOLID SPHERES BY PENETRATION OF A STACK OF SHEETS OF PAPER	5
INTRODUCTION	5
STOPPING OF A SPHERE BY PENETRATING PAPER	6
LENGTH OF PATH THROUGH PAPER TO STOP A SPHERE	12
Duration of Period of Penetration	12
Length of Path through the Paper to Stop Sphere	12
Length of Path of Sphere in Stacked Sheets of Paper	13
LIMITED EVALUATION OF CONSTANTS BY COMPARISON OF DERIVED EQUATION WITH AN EXPERIMENT	18
DISCUSSION OF EVALUATION AND SIGNIFICANCE OF CONSTANTS IN THE DERIVED EQUATIONS	21
Constants Involved in the Evaluation	21
Omission of u_o and u_f from the Evaluation of the Constants	22
Evaluation of Constants with Restraints on the Variables	24
Discussion of the Values of the Constants as Determined by One Experiment	25
PHASE TWO	27
EXPANSION OF A SPHERE OF PLASMA WITH DIFFERENT INITIAL ENERGIES	27
INTRODUCTION	27
GENERAL BASIS FOR CALCULATION OF THE EXPANSION OF A SPHERE OF PLASMA	29

TABLE OF CONTENTS (Continued)

	Page
Microfields in Dense Plasmas	29
Equation of State Employed for Subsequent Calculations	30
Limitation of this Equation of State	33
PRESENTATION OF RESULTS	37
General Statement of the Problem	37
Expansion of a Plasma with an Initial Energy of 44.45 eV per Atom	40
Expansion of a Plasma with an Initial Energy of 20.8 eV per Atom	49
Expansion of a Plasma with an Initial Energy of 7.136 eV per Atom	54
DISCUSSION OF THE SIGNIFICANCE OF THE RESULTS FROM THE EXPANSION OF A PLASMA	56
PHASE THREE	62
ADAPTATION OF THE COMPUTER PROGRAM TO A SOLUTION FOR METEOROID BUMPER PENETRATION	62
INTRODUCTION	62
TECHNIQUE TO DETERMINE MOMENTUM AT BOTTOM SURFACE OF THIN PLATE	63
ENERGY FOR HYPERVELOCITY SEPARATION OF FRAGMENTS OF THIN ALUMINUM PLATE	64
APPENDIX A	69

LIST OF FIGURES

Page

Figure 1. Illustration of Material Collected ahead of Sphere 22

Figure 2. Equation of State Plotted for Hydrogen as a Log-log Relation between the Electron Density Vs the Mass Density for a Total Average Energy of 2 eV per Atom in the Lower Graph 35

Figure 3. A Log-log Plot of Electron Density against the Mass Density for a Hydrogen Plasma 38

Figure 4. Density and Average Ionization Variation with the Radius (44.5 - .68) 41

Figure 5. Density and Average Ionization Variation with the Radius (44.5 - 1.3) 43

Figure 6. Density and Average Ionization Variation with the Radius (44.5 - 2.0) 44

Figure 7. Density and Average Ionization Variation with the Radius (44.5 - 2.7) 45

Figure 8. Density and Average Ionization Variation with the Radius (44.5 - .57). 47

Figure 9. Semilogrithmic Scale of Temperature and Pressure Variation with the Radius (44.5 - 5.9) 48

Figure 10. Density and Average Ionization Variation with Temperature (20.8 - 1.1) 50

Figure 11. Density and Average Ionization Variation with the Radius (20.8 - 2.26) 51

Figure 12. Density and Average Ionization Variation with Radius (20.8 - 3.4) 52

Figure 13. Density and Average Ionization Variation with Radius (20.8 - 4.5) 53

Figure 14. Density and Average Ionization Variation with Radius (20.8 - 9.8) 55

LIST OF FIGURES (Continued)

Page

Figure 15. Density and Average Ionization Variation with Radius (7.13 - 4.9) 57

Figure 16. Density and Average Ionization Variation with Radius (7.13 - 7.0) 58

Figure 17. A Typical Graph of the Performance of the Computer Program for the Impact of a Sphere of Rock (Quartz) on a Thin Plate of Aluminum 65

QUARTERLY REPORT

Contract No. NAS8-25055

October 1, 1971, through March 31, 1972

FINAL REPORT

STUDY OF DENSE ALUMINUM PLASMA

to

National Aeronautics and Space Administration
George C. Marshall Space Flight Center
Space Sciences Laboratory
Physics and Astrophysics Division, Astrophysics Branch
Marshall Space Flight Center, Alabama

from

Research Institute
Division of Graduate Programs and Research
The University of Alabama in Huntsville
P. O. Box 1247
Huntsville, Alabama 35807

by

F. C. TODD

STATUS OF STUDIES ON BUMPER PLATE PENETRATION AND SUBSEQUENT PHENOMENA

SURVEY OF SCOPE OF THE PROJECTS

Two closely associated projects are being solved with special consideration on the manner in which they interlock. The overall project is to obtain a computer program for the penetration of a thin plate of aluminum, i.e. a bumper plate, by a sphere of rock, i. e. a quartz sphere. In addition to the penetration of the plate, the solution is to predict the shape of the ejected cone of plasma with entrained aluminum fragments and perhaps some quartz fragments. A semi-empirical relation is sought to predict the ablation of the fragments to nothing as the fragments penetrate a stack of sheets of paper.

Finally, the cone of plasma impacts on the stack of paper sheets and the shock pressure is attenuated by the counter flow of the degradation products from the decomposition of the paper by the hot plasma.

Phases from both projects are reported. One project covers the initial impact, the crushing of the sphere of rock, the break up of the aluminum sheet and the conversion of the sufficiently shock-compressed regions of rock and aluminum into a plasma. The other project considers the ejection of a cone of plasma with entrained particles from the impact zone, its expansion as it traverses a region of free space and its impact on a stack of paper sheets. The ablation of fragments in penetrating a stack of paper sheets is a part of the last project. With this interlocking of the problems, the key study relates to the penetration of the plate and the ejection of cone of plasma. Problems in other phases must await the solution to this specific phase. This specific phase is a part of the proposed M.S. thesis for Mr. Mark Hooker.

At the initiation of these projects, a computer program was available which gave good results for the formation of a crater by the hypervelocity impact of a sphere of rock on a thick slab of aluminum. It was proposed to adapt the solution for the crater formation to obtain a computer program for the first part of the penetration of the thin plate. It is believed that a computer solution cannot be wirtten, without very special corrections, for the entire impact which includes the penetration of the bumper plate and the egress of the products of the impact on the bumper plate. The reason is that the aluminum of the bumper plate is ruptured by tension. At the instant of rupture, the continuum fails and all of the equations fail since they are only valid in a continuum. After a "hand" correction, the computer solution may proceed.

Both projects were tentatively assumed to require two years for a complete solution. This final report is written midway of the study, and is, of necessity, more of a long progress report than of a final report. Without reference to the separation of the projects, the overall study may be roughly divided into the following phases. These following phases are identified with the phase in this report which treats this subject.

(1) Adaptation of the available computer program for the formation of a crater to a program for the start of the penetration of a bumper plate. This phase is in progress and the program is discussed under Phase 3 of this report.

(2) The technique for making the "hand" corrections when the continuum is ruptured. This subject is under intensive study and a proposal is being formulated to continue the work next year. The discussion in Phase Three treats this subject, but does not enter into the subject in detail.

(3) After sufficient compression up the Hugoniot curve, the adiabatic expansion will leave sufficient energy in the material so the material is properly classified as a plasma. The material which egresses from the impact zone is a plasma with entrained pieces of aluminum and rock (quatz). The expansion of a high energy plasma is discussed in Phase Two of this report. A different equation of state is required for a short density range from solid density to 1/100 to 1/1000 of solid state density. After the insertion of this correction, which is available, the plasma calculation can be extended to solid state densities and to much lower energies.

(4) The computer program for the formation of a crater requires many corrections for the penetration of a thin plate. Many of the corrections have been made. It is believed at this time, that corrections which arise from the interactions at the boundary between the aluminum and the penetrating rock are the most important ones which remain uncorrected. The work that is reported in Phase Three presents the present status of work on this program.

(5) The plasma that is ejected from the bumper plate contains many fragments of aluminum and rock. The fragments are usually around the circumference of the plasma. One phase of a contract is to derive a semi-empirical equation to represent the penetration of the fragments into a stack of sheets of a special paper. After a second trial at the derivation, an analytical equation was derived and compared with the results of one experiment. Since there are three major constants in the solution, the evaluation of all three constants is not possible with the results from one experiment. The results of many more experiments are available, but the author only accepted the results from one at the start of this program. Many more experiments and some fitting of equations is necessary in order to obtain a semi-empirical equation. This work is considered in Phase One of this report.

In the following report, there are three major phases discussed. These three phases do not exactly coincide with the above breakdown into five parts that are discussed in this introduction to this report. In the preceding list of five parts, the phase in the report to which the discussion most nearly relates is mentioned. The phases in the report are Ablation of a Solid Sphere by Penetration of a Stack of Sheets of Paper, Expansion of a Sphere of Plasma with Different Initial Energies, and Adaptation of the Computer Program to a Solution for Meteoroid Bumper Penetration.

PHASE ONE

ABLATION OF SOLID SPHERES BY PENETRATION OF A STACK OF SHEETS OF PAPER

INTRODUCTION

In the Third Quarterly Report, the complete ablation of a sphere of rock by penetrating sheets of paper was considered. The force to decelerate the sphere was assumed to have the form of Stoke's law for the frictional force on a sphere falling through a viscous liquid. The solution was obtained, with some difficulty. On comparison with experiment, the coefficient of viscosity was found to be ridiculously low. It was less than the viscosity of water. Stoke's law assumes that the losses are distributed through a substantial volume, and the affected volume extends from the surface of the sphere for some distance into the paper. The above result was interpreted to mean that the actual losses are very close to the surface of the sphere. On this assumption, a new equation was formulated for the forces that oppose penetration of the sphere through the paper.

In this report, the equation for losses near the surface of the sphere is restated with a little explanation of the basis on which it was formulated. A solution is eventually obtained in terms of three basic constants. With the results from one experiment, it is not possible to evaluate the basic constants. It is feasible to evaluate a ratio between two critical constants and to evaluate this ratio over the range of values which are assumed to be of interest.

The derivation of this equation is given in detail. If there is sufficient financial support for the author to complete the problem, the sponsor will have no difficulty in employing experimental results in order to ascertain the merit of the equation. At this time, the author wishes to acknowledge the exceedingly helpful assistance of a graduate student, Mr. Mark Hooker. Mr. Hooker is working on a thesis to fulfill part of the requirements for his M.S. degree. His assistance to the author was most valuable in checking equations and signs. He was also most helpful in discussing the study. In addition, Hooker is entirely responsible for the technique by which the variables were separated in order to calculate u in terms of r.

The author's original concept of the plug, ahead of the sphere, was that it had the shape of a cylinder. As shown in Figure 1, the plug is really a very thin shell that is ahead of the sphere. From this difference, there should be a numerical constant inserted in the first term on the right of the equality sign. Instead of the term $\pi r^2 \ell r \rho_1 u$ for the mass of a cylinder, the term should read $2 \pi r^2 \ell r \rho_1$ for the mass of a thin hemispherical shell.

STOPPING OF A SPHERE BY PENETRATING PAPER

In the third progress report, it was shown that an absurdly low value is obtained for the viscosity, η, when the drag on a penetrating sphere is represented by Stoke's law. The low value of η indicates that the actual losses are concentrated very near the penetrating sphere. In the derivation of Stoke's law, a particle in linear motion is restrained by viscous forces in a liquid with laminar, or "streamline" flow. This distributes the frictional losses through a considerable volume that surrounds the path of the penetrating sphere. The low value of η from the application of Stoke's law to the experimental data indicates that the loss cannot be in a large volume but must be in a small volume and this requires that the losses be very close to the penetrating sphere.

In order to confine the loss to close proximity to the sphere, a new relation is sought. In this relation, the losses are represented by two terms; (1) the force to accelerate the material in a short column ahead of the sphere to the velocity of the sphere and (2) the force necessary to move the sphere and column against the restraining, frictional type forces that surround it and any force that is required to shear the material. The first term depends on the instantaneous projected area of the sphere. In contrast, the second term is the shear and friction of moving the accelerated material into the stack of paper. In words, the equation may be written

Force to decelerate sphere	=	Force to accelerate a a column of thickness ℓ and area πr^2	plus	Force to shear and force a plug through the hole

$$\frac{\partial\left(\frac{4}{3}\pi r^3 \rho u\right)}{\partial t} = \frac{\partial(\pi r^2 \ell_r \rho_1 u)}{\partial t} + 2\pi r \ell_r S \frac{\partial u}{dt}$$

In the first term on the left of the equality, $\frac{4}{3}\pi r^3 \rho$ is the instantaneous mass of the penetrating sphere, when ρ is the density of aluminum. When the mass is multiplied u, this term becomes the momentum. The differential of the momentum is the force in dynes. Similarly, $\pi r^2 \ell_r \rho_1$ is the mass of a circular plug of the paper material that is accelerated ahead of the entering sphere. It is believed that this material piles up to an undetermined thickness, ℓ_r, and then permits the sphere to squeeze through it with added friction which is given in the last term. By multiplying the first term on the right of the equality by the

velocity, u, the momentum is obtained and the rate of change of momentum with time is a force in dynes.

The final term on the right is the effective frictional force as the circumference of the sphere is forced through the plug of material that is formed according to the first term on the right. The force in dynes is obtained by multiplying by the acceleration. The term, S, is the force in grams/cm^2 of wall area of the plug which has a circumference of $2\pi r$ and a length of ℓr.

The variables in the equation may be obtained in a more generally applicable form

$$\frac{4}{3}\pi\rho u 3r^2\frac{dr}{dt} + \frac{4}{3}\pi\rho r^3\frac{du}{dt} = \pi\ell\rho_1 3r^2 u\frac{dr}{dt} + \pi\ell\rho_1 r^3\frac{du}{dt} + 2\pi\ell S r^2\frac{du}{dt}$$

Partially collecting terms

$$\left(\frac{4}{3}\pi\rho - \pi\ell\rho_1\right)3r^2 u\frac{dr}{dt} = \left(-\frac{4}{3}\pi\rho r^3 + \pi\ell\rho_1 r^3\right)\frac{du}{dt} + 2\pi\ell S r^2\frac{du}{dt}$$

Continue to collect terms

$$\left(\frac{4}{3}\pi\rho - \pi\ell\rho_1\right)3r^2 u\frac{dr}{dt} = \left(\pi\ell\rho_1 r^3 + 2\pi\ell S r^2 - \frac{4}{3}\pi\rho r^3\right)\frac{du}{dt}$$

Solve for $\frac{dr}{dt}$

$$\frac{dr}{dt} = \frac{\pi\ell\rho_1 r^3 + 2\pi\ell S r^2 - \frac{4}{3}\pi\rho r^3}{\frac{4}{3}\pi\rho\cdot 3r^2 u - \pi\ell\rho_1 3r^2 u}\frac{du}{dt}$$

This equation may be rewritten in a form for use in the calculations.

$$\frac{dr}{dt} = \frac{\ell\rho_1 r + 2\ell S - \frac{4}{3}\rho r}{4\rho - 3\ell\rho_1}\frac{1}{u}\frac{du}{dt}$$

Solution of Simultaneous Differential Equations for Relation between u and r

With the differential equation that is derived above and with the two others that were derived in the third progress report, there are three differential equations to solve simultaneously for the three independent variables r, u and Q. These simultaneous

differential equations are collected here.

$$\frac{dQ}{dt} = 4\pi r^2 D \tag{1}$$

This equation comes from the definition for the linear flow of heat. The term $\frac{dQ}{dt}$ is the flow of heat in calories per second. The term, D, is an "adjustable constant" which replaces the term

$$K\frac{dT}{dr}$$

where K is the thermal conductivity of the bunched and compressed material which is just outside the surface of the sphere. The term $\frac{dT}{dr}$ is the effective temperature gradient in this material.

The second differential equation was derived in the preceding section. This equation was derived from the forces acting on the sphere on the assumption of "localized forces". It has the form

$$\frac{dr}{dt} = \frac{\ell\rho_1 r + 2\ell S - \frac{4}{3}\rho r}{4\rho - 3\ell\rho_1}\,\frac{1}{u}\,\frac{du}{dt} \tag{2}$$

In this relation, r is the instantaneous radius of the sphere that is penetrating the paper, ℓr is the effective thickness of the "plug" of paper pushed ahead by the sphere, S is the shear force which opposes the movement of the plug, ρ is the density of aluminum and ρ_1 is the density of the paper. The instantaneous velocity at any instant is u.

From the conservation of energy by equating the initial kinetic energy to the losses of energy, the following equation was obtained in units of calories per second.

$$\frac{dQ}{dt} = -1.6685 \times 10^{-8}\,\rho\left(3r^2u^2\,\frac{dr}{dt} + 2r^3\,u\,\frac{du}{dt}\right) \tag{3}$$

In this relation, the values of ρ, r, u and t are the same as in the preceding equations.

Eliminate variables in order to simplify the equations. Start by equating equations (1) and (3) in order to eliminate $\frac{dQ}{dt}$

$$4\pi r^2 D = -1.6685 \times 10^{-8} \rho \left(3r^2 u^2 \frac{dr}{dt} + 2r^3 u \frac{du}{dt}\right)$$

This equation will eventually be solved for $\frac{dr}{dt}$ and $\frac{du}{dt}$. As the first step, the equation may be formed into the sum of two differentials.

$$3r^2u^2 \frac{dr}{dt} + 2r^3 u \frac{du}{dt} = -\frac{4\pi r^2 D}{1.6685 \times 10^{-8} \rho}$$

Divide this equation by $3r^2u^2$ and transpose one term to the right side of the equality

$$\frac{dr}{dt} = -\frac{4\pi D}{1.6685 \times 10^{-8} \rho} \frac{1}{3u^2} - \frac{2}{3} \frac{r}{u} \frac{du}{dt} \tag{4}$$

Among the three simultaneous equations for solution, there is another differential equation for $\frac{dr}{dt}$. This is Equation 2 above and is rewritten here for ready reference.

$$\frac{dr}{dt} = \frac{\ell \rho_1 r + 2\ell S - \frac{4}{3} \rho r}{4\rho - 3\ell \rho_1} \frac{1}{u} \frac{du}{dt} \tag{2}$$

The terms on the right hand side in Equations 4 and 2 may be equated to each other since both are equal to $\frac{dr}{dt}$.

$$\frac{\ell \rho_1 r + 2\ell S - \frac{4}{3} \rho r}{4\rho - 3\ell \rho_1} \frac{1}{u} \frac{du}{dt} = -\frac{4\pi D}{1.6685 \times 10^{-8} \rho} \frac{1}{3u^2} - \frac{2}{3} \frac{r}{u} \frac{du}{dt}$$

Rearrange the terms in order to factor out $\frac{du}{dt}$

$$\left(\frac{\ell \rho_1 r + 2\ell S - \frac{4}{3} \rho r}{4\rho - 3\ell \rho_1} + \frac{2}{3} r\right) \frac{1}{u} \frac{du}{dt} = -\frac{1}{3u^2} \frac{4\pi D}{1.6685 \times 10^{-8} \rho}$$

In order to simplify this relation, multiply through by -3.

$$\left(\frac{(4\rho - 3\ell \rho_1) r - 6\ell S}{4\rho - 3\ell \rho_1} - 2r\right) u \frac{du}{dt} = \frac{4\pi D}{1.6685 \times 10^{-8} \rho}$$

In order to further simplify the relation, introduce the constants P_1, P_2, and P_3 where the constants are defined by the following relations

$$P_1 = \frac{4\pi D}{1.6685 \times 10^{-8}}; \quad P_2 = 4\rho - 3\ell \rho_1; \quad P_3 = -6\ell S$$

Introduce the new constants and further simplify

$$\left(\frac{rP_2 + P_3}{P_2} - 2r\right) u \frac{du}{dt} = P_1$$

Obtain a common denominator and rearrange the terms

$$\left(\frac{P_3 - rP_2}{P_2}\right) u \frac{du}{dt} = P_1 \qquad (5)$$

This is an equation for $\frac{du}{dt}$ in terms of the variables u and r and of the constants P_1, P_2 and P_3.

The next step is to use the same two Equations 4 and 2 in order to obtain an expression for $\frac{dr}{dt}$. Proceed by obtaining an equation for $\frac{du}{dt}$ from Equation 4.

$$\frac{2}{3}\frac{r}{u}\frac{du}{dt} + \frac{dr}{dt} = -\frac{1}{3u^2} P_1$$

$$\frac{du}{dt} = -\frac{3u}{2r}\frac{dr}{dt} - \frac{3u}{2r}\frac{1}{3u^2} P_1 \qquad (a)$$

Now consider Equation 2 and modify it in order to obtain an equation with the constants inserted. With a slight rearrangement, Equation 2 becomes

$$\frac{dr}{dt} = \frac{-3}{-3}\frac{\ell\rho_1 r - \frac{4}{3}\rho r + 2\ell S}{4\rho - 3\ell\rho_1}\frac{1}{u}\frac{du}{dt} = -\frac{1}{3}\frac{rP_2 + P_3}{P_2}\frac{1}{u}\frac{du}{dt}$$

Rearrange the above relation in order to solve for $\frac{du}{dt}$

$$\frac{du}{dt} = -3u\frac{P_2}{rP_2 + P_3}\frac{dr}{dt} \qquad (b)$$

In order to eliminate $\frac{du}{dt}$, equate Equation a to Equation b.

$$-\frac{3udr}{2rdt} - \frac{3u}{2r}\frac{1}{3u^2} P_1 = -3u\frac{P_2}{rP_2 + P_3}\frac{dr}{dt}$$

Divide both sides of the equation by -3 and rearrange terms

$$\left(+\frac{1}{2r} - \frac{P_2}{rP_2 + P_3}\right)\frac{dr}{dt} = -\frac{1}{6ru^2} P_1$$

Continue to simplify this relation

$$-3u^2\frac{P_3 - rP_2}{P_3 + P_2}\frac{dr}{dt} = P_1 \qquad (6)$$

Starting with Equations 4 and 2, $\frac{dr}{dt}$ is obtained in Equation 6 as a function of the variables u and r and of the constants P_1, P_2 and P_3. In Equation 5, $\frac{du}{dt}$ was obtained as a function of the same variables u and r and of the same constants. Equations 5 and 6 were obtained from Equations 4 and 2. No variables or constants have been eliminated but the equations are in a different form.

From an inspection of the relations in Equations 5 and 6, each equation may be solved for the constant, P_1. The two equations may then be equated to each other by the elimination of the variable, P_1.

$$\frac{P_3 - rP_2}{P_2} \, u \frac{du}{dt} = -3u^2 \frac{P_3 - rP_2}{P_3 + rP_2} \frac{dr}{dt}$$

After simplifying this relation, the following form is found

$$-\frac{1}{3u} \frac{du}{dt} = \frac{1}{\frac{P_3}{P_2} + r} \frac{dr}{dt}$$

In this relation, the variables are separated and integration may proceed at once

$$-\frac{1}{3} \ln u = \ell n \left(\frac{P_3}{P_2} + r \right)$$

$$\frac{1}{u^{\frac{1}{3}}} = r + \frac{P_3}{P_2}$$

A relation between u and r is necessary in order to evaluate measurable quantities in the experiment such as the length of path to stop the penetrating particle, or the length of path to completely ablate the sphere.

In the above relation between u and r, a constant of integration should be added. From the manner in which the equation was integrated, the constant could be inserted in several ways. In one method, the equation may be rewritten as

$$\frac{1}{(Cu)^{\frac{1}{3}}} = r + \frac{P_3}{P_2}$$

In this case, the constant, C, may be considered as a multiple of the velocity, u. There will be no other reference to C until the discussion of the evaluation of the constants.

LENGTH OF PATH THROUGH THE PAPER TO STOP A SPHERE

(Duration of Period of Penetration)

From the relation between u and r that was obtained in the preceding section, the length of path through the stacked sheets of paper may be calculated. There are two solutions for the length of path: (a) The length of path for complete ablation of the entering sphere. This occurs when there is an excess of the initial kinetic energy. (b) The length of path through the stacked sheets of insulation to stop the sphere with a finite, final radius, r_f. No entering sphere in the experimental range of sizes is expected to reach the rear surface of the stack of sheets of paper. If the solution from this study proves to be adaptable to obrain reliable results, then it would be desirable to obtain a solution for the velocity and radius of a sphere which is either oversize and has excessive initial energy in order to predict the radius of the sphere and the velocity at the back plate after it has penetrated the insulation.

In order to make the desired computations, it is desirable to select three equations from the preceding section as the foundation for the studies in this section. The first of the three relations is the relation for $\frac{du}{dt}$ when $\frac{dr}{dt}$ is eliminated from the equation

$$\frac{P_3 - rP_2}{P_2} \; u \frac{du}{dt} = P_1 \tag{5}$$

The second of the three equations is the relation for $\frac{dr}{dt}$ when $\frac{du}{dt}$ is eliminated from the equation

$$-3u^2 \frac{P_3 - rP_2}{P_3 + P_2} \frac{dr}{dt} = P_1 \tag{6}$$

The final equation of the three equations is the relation between r and u which is obtained from the two preceding equations

$$\frac{1}{u^{\frac{1}{3}}} = r + \frac{P_3}{P_2} \tag{7}$$

Length of Path of Sphere in Stacked Sheets of Paper

From the three Equations 5, 6 and 7, it is desired to calculate the length of path of the penetrating sphere in the stacked paper insulation. There are two distinct problems for which a solution is required. The length of path is desired (a) to stop the sphere by ablating it to nothing and (b) to stop the sphere by ablating it down to an approximate sphere of finite radius, r_f. Start with Equation 7 but rewrite it in a form that gives the value of u

$$u = \frac{1}{\left(r + \frac{P_3}{P_2}\right)^3}$$

This relation may be written in another form by recalling that u is $\frac{ds}{dt}$ where Δs is an element of length along the path of penetration of the sphere. The new form of the above equation is

$$\left(r + \frac{P_3}{P_2}\right)^3 \frac{ds}{dt} = 1$$

Introduce a new independent variable, r.

$$\left(r + \frac{P_3}{P_2}\right)^3 \frac{ds}{dr}\frac{dr}{dt} = 1$$

This equation may be rewritten in still another form

$$\left(r + \frac{P_3}{P_2}\right)^3 \frac{dr}{dt} = \frac{dr}{ds}$$

The value of $\frac{dr}{dt}$ is known from Equation 6 and on substitution, the relation becomes

$$\left(r + \frac{P_3}{P_2}\right)^3 \left(-\frac{P_1}{3u^2}\right)\left(\frac{P_3 + rP_2}{P_3 + rP_2}\right) = \frac{dr}{ds}$$

Now insert the value of u^2 from Equation 7

$$\left(\frac{P_2r + P_3}{P_2}\right)^9 \left(-\frac{P_1}{3}\right)\left(\frac{P_2r + P_3}{P_2}\right)^8 \frac{(P_2r + P_3)}{(P_3 - rP_2)} = \frac{dr}{ds}$$

Simplify the above relation by collecting terms

$$\frac{(P_2r + P_3)^{10}}{(P_3 - rP_2)}\left(-\frac{P_1}{3P_2^9}\right) = \frac{dr}{ds}$$

Separate variables and put in a form for integration

$$-\frac{P_1}{3(P_2)^9}\,ds = \frac{P_3}{(P_2 r + P_3)^{10}}\,dr - P_2\,\frac{r\,dr}{(P_2 r + P_3)^{10}} \tag{8}$$

Since the preceding integral is rather involved, the terms on the right are integrated one by one. After integration, the separate solutions are reinserted into a single equation. Consider only the terms in the fractions that are involved in the first term on the right in the last equation above. The expression to be integrated is

$$\int \frac{1}{(P_3 + rP_2)^{10}}\,dr$$

From a table of integrals, there is a substitution for this type of term. The substitution requires that $y \equiv a + bx$, then tables of integrals show that the following relation exists

$$\int (a + bx)^m\,dx = \frac{1}{b}\int y^m\,dy$$

For the integral under consideration, $m = -10$, $a = P_3$, $b = P_2$. With these substitutions

$$\int \frac{dr}{(P_3 + P_2 r)^{10}} = \frac{1}{P_2}\int (P_3 + P_2 r)^{-10}\,d\,(P_3 + P_2 r) = -\frac{1}{9P_2}\,\frac{1}{(P_3 + P_2 r)^9}$$

The involved terms in the second expression for integration are

$$\int \frac{r\,dr}{(P_3 + P_2 r)^{10}}$$

From a table of integrals, there is a substitution when the following identity hold for this type of equation, $y \equiv a + bx$. The relation from the table of integrals is

$$\int \frac{x^n\,dx}{(a + bx)^m} = \frac{1}{b^{n+1}}\int \frac{(y - a)^n}{y^m}\,dy$$

For the integral under consideration, the following relations hold: $m = 10$, $n = 1$, $a = P_3$ and $b = P_2$

With these substitutions

$$\int \frac{r\,dr}{(P_3 + P_2 r)^{10}} = \frac{1}{P_2^{1+1}}\int \frac{(y - a)}{y^{10}}\,dy = \frac{1}{P_2^2}\int y^{-9}\,dy - \frac{P_3}{P_2^2}\int y^{-10}\,dy$$

$$= -\frac{1}{8P_2^2}\, y^{-8} + \frac{P_3}{9P_2^2}\, y^{-9}$$

$$= -\frac{1}{8P_2^2}\,\frac{1}{(P_3 + P_2 r)^8} + \frac{P_3}{9P_2^2\,(P_3 + P_2 r)^9}$$

Now collect all of the terms and reinsert them in Equation 8. For an integration without limits, such as this one, a constant of integration, C, must be added after the simplification is completed.

$$-\frac{P_1}{3(P_2)^9}\, s = -\frac{P_3}{9P_2}\,\frac{1}{(P_3 + P_2 r)^9} + \frac{1}{8P_2}\,\frac{1}{(P_3 + P_2 r)^8} - \frac{P_3}{9P_2}\,\frac{1}{(P_3 + P_2 r)^9}$$

Simplify by several steps, change signs through the equation, multiply by P_2, and combine terms

$$\frac{P_1}{3(P_2)^8}\, s = \frac{P_3}{(P_3 + P_2 r)^9}\left[\frac{1}{9} + \frac{1}{9}\right] - \frac{1}{8}\,\frac{1}{(P_3 + P_2 r)^8}$$

Put the equation in its final form and add the constant of integration, C

$$\frac{P_1}{3(P_2)^8}\, s = \frac{2P_3}{9}\,\frac{1}{(P_3 + P_2 r)^9} - \frac{1}{8}\,\frac{1}{(P_3 + P_2 r)^8} + C \qquad (9)$$

The preceding relation, Equation 9, is a general equation with the length of path, s, and the radius, r, of the sphere. This equation may be evaluated between several limits. Two sets of these limits are of particular merit in evaluating the undetermined "constants" that are in this equation. One set of limits corresponds to a sphere of radius, r_o, that enters the stack of paper at the start of the path of penetration, $s = 0$, and is completely ablated, $r = 0$, after a path length, s_f. The second set of limits correspond to a sphere that is not completely ablated and stops in the stack of paper. This set of limits corresponds to a sphere of radius, r_o, that enters the stack of paper, $s = 0$, and

is ablated to a radius, d, after traveling along the path of penetration for a distance, s_d. In other words, a portion of the entering particle is found in the stack of paper at a distance, s_d, from the entrance of the particle into the stack of paper.

The first set of limits, which are to be inserted, is for the spherical particle which is completely ablated as it penetrates the stack of sheets of paper. The limits for integration for this set of conditions are: initial conditions, $s = 0$ when $r = r_o$; and the final set of conditions, $s = s_f$ when $r = 0$. When limits of integration are inserted, there is no need for the constant, C. Omit this constant and insert the above limits of integration into Equation 9.

$$\frac{P_1}{3(P_2)^8} s \Bigg|_{s=o}^{s=s_f} = \frac{2P_3}{9} \frac{1}{(P_3 + P_2 r)^9} \Bigg|_{r=r_o}^{r=o} - \frac{1}{8} \frac{1}{(P_3 + P_2 r)^8} \Bigg|_{r=r_o}^{r=o}$$

On the insertion of these limits, the following relation is obtained.

$$\frac{P_1}{3(P_2)^8} s_f = \frac{2P_3}{9} \left[\frac{1}{(P_3)^9} - \frac{1}{(P_3 + P_2 r_o)^9} \right] - \frac{1}{8} \left[\frac{1}{(P_3)^8} - \frac{1}{(P_3 + P_2 r_o)^8} \right]$$

Separate the terms with r_o from the other terms

$$= \frac{1}{8} \frac{P_3 + P_2 r_o}{(P_3 + P_2 r_o)^9} - \frac{2P_3}{9} \frac{1}{(P_3 + P_2 r_o)^9} + \frac{2P_3}{9(P_3)^9} - \frac{1}{8} \frac{1}{(P_3)^8}$$

Collect and simplify the terms in this relation

$$= \frac{1}{(P_3 + P_2 r_o)^9} \left[-\frac{7}{72} P_3 + \frac{1}{8} P_2 r_o \right] + \frac{7}{72} \frac{1}{(P_3)^8}$$

Solve for $P_1 s_f$ and continue to simplify the terms

$$P_1 s_f = \frac{(P_2)^8}{24} \frac{9P_2 r_o - 7P_3}{(P_3 + P_2 r_o)^9} + \frac{7}{24} \left(\frac{P_2}{P_3} \right)^8 \qquad (10)$$

To recapitulate, this solution is for a sphere of radius, r_o, which enters a stack of paper sheets at a length of path through the paper of $s = 0$. After traveling through the sheets of paper for a distance, s_f, the sphere is completely ablated. For comparison with this solution, derive the other practical example in the next paragraph.

Consider the other set of practical limits when an entering sphere is stopped in the stack of paper before it is completely ablated. The limits of integration for this set of conditions are

$$s = 0 \text{ when } r = r_o$$

$$s = s_d \text{ when } r = d$$

In this set of relations, s_d is the length of path through a stack of sheets of paper before the sphere is stopped with a radius, d. The integral with the limits of integration becomes

$$\frac{P_1}{3(P_2)^8} s \Bigg|_{s=o}^{s=s_d} = \frac{2P_3}{9} \frac{1}{(P_3 + P_2 r)^9} \Bigg|_{r=r_o}^{r=d} - \frac{1}{8} \frac{1}{(P_3 + P_2 r)^8} \Bigg|_{r=r_o}^{r=d}$$

With the limits inserted, the relation becomes

$$\frac{P_1}{3(P_2)^8} s_d = \frac{2P_3}{9} \left[\frac{1}{(P_3 + P_2 d)^9} - \frac{1}{(P_3 + P_2 r_o)^9} \right] - \frac{1}{8} \left[\frac{1}{(P_3 + P_2 d)^8} - \frac{1}{(P_3 + P_2 r_o)^8} \right]$$

Separate these terms into two groups according to d and r_o, which are the final and the initial radii of the penetrating sphere, respectively.

$$= \frac{1}{(P_3 + P_2 d)^9} \left[\frac{2P_3}{9} - \frac{1}{8} P_3 - \frac{1}{8} P_2 d \right] - \frac{1}{(P_3 + P_2 r_o)^9} \left[\frac{2P_3}{9} - \frac{1}{8} P_3 - \frac{1}{8} P_2 r_o \right]$$

Continue to simplify and collect the terms in the above relation

$$= \frac{1}{72} \frac{7P_3 - 9P_2 d}{(P_3 + P_2 d)^9} - \frac{1}{72} \frac{7P_3 - 9P_2 r_o}{(P_3 + P_2 r_o)^9}$$

Solve this relation for $P_1 s_d$ and simplify the terms

$$P_1 s_d = \frac{(P_2)^8}{24} \frac{7P_3 - 9P_2 d}{(P_3 + P_2 d)^9} - \frac{(P_2)^8}{24} \frac{7P_3 - 9P_2}{(P_3 + P_2 r_o)^9} \qquad (11)$$

The preceding two Equations 10 and 11 are for the complete and the partial ablation, respectively, of a high velocity sphere which enters a stack of sheets of paper. One set of experimental data is available to evaluate the constants in Equation 10 but no data is available to evaluate the constants in Equation 11.

LIMITED EVALUATION OF CONSTANTS BY COMPARISON OF DERIVED EQUATION WITH AN EXPERIMENT

After the analytical form of the above equation is obtained, it is desirable to evaluate the constants. At this stage, over optimism must be avoided. The general equation will probably fit a very restricted range of the data and the equation must receive a major modification before it may be applied to the general problem. Since there are three basic constants, P_1, P_2 and P_3, these cannot possibly be determined by the results from a single test. (In order to keep close contact with the Sponsor, the author has only accepted the results from a single test up to this time.) With a single experiment, only a range of ratios may be obtained between the most sensitive "constants". In this section, this ratio is obtained for adjustments in two sensitive "constants". The first step will be to restate the results of the one experimental test which has been accepted by the author.

In the third Quarterly Progress Report, the values are given for one experimental test. This information is for Experimental Shot No. 203. The incident particle was an aluminum sphere with a weight of 0.010 grams. The initial diameter of the sphere was 0.075 inches, or 0.1905 cm. For use in the derived equation, the initial radius, r_o, was 0.09525 cm. The initial velocity was 6.15 km/sec, or 6.15×10^5 cm/sec. The length of path through the stack of paper sheets in order to ablate the sphere was about 8 cm. The mean density of the paper was 0.4609 gms/cm^3 which is less than half of the density of water.

The derived equation employs three constants, P_1, P_2, and P_3. These constants are defined in the preceding derivations. There are actually more than three constants, but for the following evaluation, it will be found that the most significant adjustable constants are in P_1 and in $P_3 + P_2 r_o$. It is obvious that a single measurement cannot evaluate these three constants. It can only approximately determine a ratio between the two most sensitive "constants" among those which determine P_1, P_2 and P_3.

The two most sensitive "constants" are ℓS and D. The active constant, ℓS, is the product of ℓ times a combination of the average shear and the average friction. The method of combination of these two factors is not known. The value, ℓ, is defined by means of the product ℓr where this value is the effective length, parallel to the direction of motion, of

the friction surface around the circumference of the penetrating sphere. In the product, ℓr, ℓ is a pure number between 0 and 1 and r is the instantaneous radius of the penetrating sphere. In other words, ℓS, is a combination that is proportional to the friction and to the shear in unknown proportions. The sensitive "constant", D, is representative of entirely different factors. It was discussed extensively in the preceding Progress Report. It is defined by the equation

$$D = K\frac{dT}{dr}$$

where K is the thermal conductivity and $\frac{dT}{dr}$ is the instantaneous radial temperature gradient. The definition applies to the region of damaged material which is between the undisturbed sheets of paper and the surface (probably molten) of the penetrating sphere.

The equation for evaluation is Equation 10 which has the form

$$P_1 s_f = \frac{(P_2)^8}{24} \frac{9P_2 r_o - 7P_3}{(P_3 + P_2 r_o)^9} + \frac{7}{24}\left(\frac{P_2}{P_3}\right)^8$$

The constants in this equation have the following values.

$$P_1 = \frac{4\pi D}{1.6685 \times 10^{-8}} \quad \text{where } D = K\frac{dT}{dr}$$

As stated above, K is the thermal conductivity of the crushed and torn material that surrounds the penetrating sphere. The temperature gradient, $\frac{dT}{dr}$, is through this same crushed material in the region which is just outside of the metal of the penetrating sphere. The numerical value in the denominator is for the purpose of converting calories and thermal conductivities into units which are compatible with the c.g.s. units in the other differential equations. The manner of obtaining this numerical value is discussed in detail in the third Progress Report. The value of D is not known and may only be estimated. A range of estimated ratios will be obtained from the experimental test.

The constant, P_2, is given by the following relation

$$P_2 = 4\rho - 3\ell\rho_1$$

The density, ρ, is the density of aluminum which is assumed to be 2.765 grams per cm^3 from various references. The density, ρ_1, is the mean density of the stack of sheets of

paper. From the experiment that is referenced, the value of ρ_1 is 0.4609 grams per cm^3. This density is less than half of the density of water.

The constant, P_3, is defined by the following relation

$$P_3 = -6\ell S$$

There is no guidance known to the author from which to select numerical values for ℓ and S. For the calculations that follow, a value of 10 grams per cm^2 is assumed for S. Then values of ℓ are assumed which give values of D which appear to be in a practical range.

The derivations of the three simultaneous, differential equations and the search for their solution has been in much more detail than is usual. This detail was added because of the great uncertainty as to the basis for the derivation. It will make it much easier to modify as comparison with experiments proceed. The insertion of numerical values is illustrated by one solution which is reproduced in Appendix A. Three solutions have been obtained for different values of ℓ which determine three values for D. These results are reported in Table I.

Table I

Values of D Calculated from Assumed Values of ℓ

ℓ	D
Pure Number	$\frac{\text{calories}}{cm^2\ sec}$
0.01	12.90
0.011	103.9
0.012	1516.

It is to be recalled that there is a minimum of three constants; P_1, P_2 and P_3. It is obvious that a single experiment cannot uniquely determine these three constants. Actually, there are more than three constants and the author has chosen two of these constants to be more important and has assumed that they vary more rapidly than the others in range of particle size and range of penetrations that are represented by the one experiment, for which data is immediately available. The choice is arbitrary and a better choice might be made. The entire subject is so uncertain that it is discussed in more detail in the next section.

DISCUSSION OF EVALUATION AND SIGNIFICANCE OF CONSTANTS IN THE DERIVED EQUATIONS

In this section, random comments are given on the evaluation of the "constants" in the derived equations by means of comparison with experimental data. The derived equation must be treated as suspected of not satisfying the experimental data. For this reason, the experimental data should be inserted in a way that will emphasize the deviation and permit the basic, differential equations to be modified in order to be more correct. As an example, K must be suspected of being a function of the velocity, u, or of the radius, r, which is essentially the same thing, in this stage of the development. Since these comments will range over a wide range of subjects, subheadings are employed although many of the subheadings may only be a paragraph in length.

Constants Involved in the Evaluation

For simplicity in integrating the differential equations, three constants are employed. These constants are P_1, P_2 and P_3. As indicated in the preceding section, these three constants represent at least 6 constants: K, $\frac{dT}{dr}$, ρ, ρ_1, ℓ and S. In practical examples, ρ and ρ_1, are known in the most general cases without conducting an experiment to evaluate them. The density of the penetrating sphere is ρ, and the average density of the stack of sheets of paper is ρ_1. Two of the constants are impossible to evaluate separately by the type of measurements that are presented in the illustration in this report. These are $K\frac{dT}{dr}$ where K is the thermal conductivity and $\frac{dT}{dr}$ is the thermal gradient in a region of thickness, Δr, which is just outside of the penetrating sphere. Minor modifications may be made in the experiments which will permit separation of these constants.

The constant, ℓ, is difficult to define. The explanation is perhaps easiest to introduce by means of a sketch which is designated as Figure 1. As the sphere penetrates, it is assumed to collect and accelerate a thickness, ℓr, of the debris from the degradation of the paper. The thickness of the added materials is ℓr where ℓ is a pure number and r is the instantaneous radius of the sphere. This thickness only covers the entering hemisphere where it is accelerated by the moving sphere. From the numerical statement of this assumption, it is to be observed that the thickness of the layer varies as the instantaneous radius of the sphere. In addition, there is a roughly cylindrical shape around the circumference of the sphere where

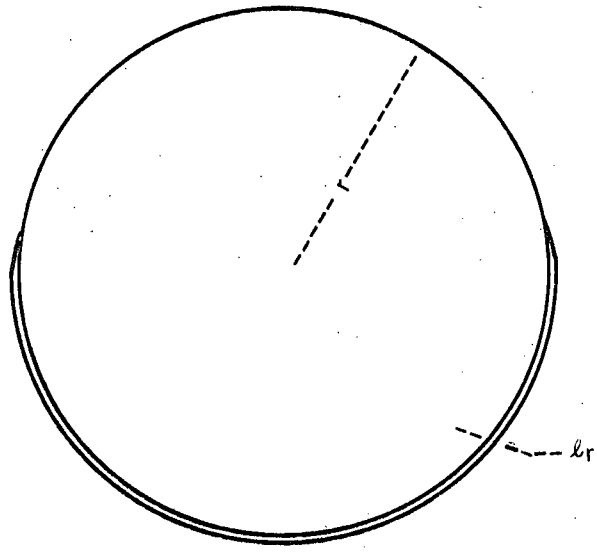

A. Enlarged Sphere for Material Collected Ahead of the Sphere.

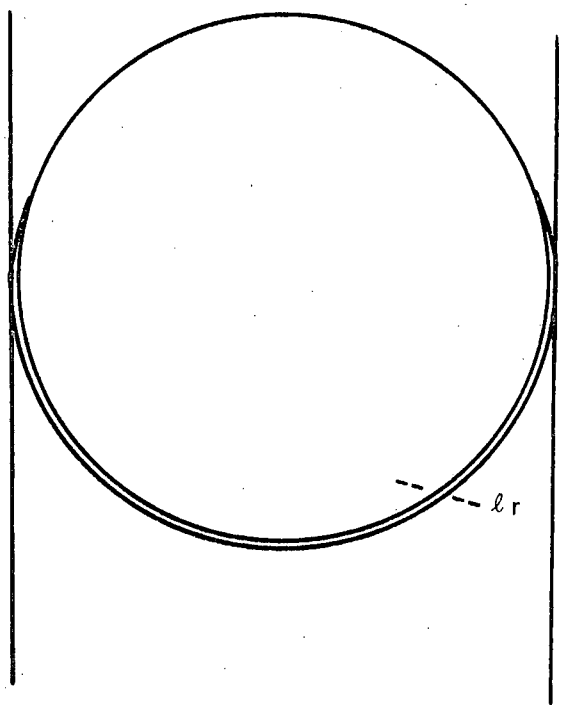

B. Cylindrical Shape for Friction and Shear Against the Wall.

Figure 1. Illustration of Material Collected Ahead of Sphere.

the crushed material that is ahead of the sphere "slides" between the largest diameter of the "instantaneous" size of the sphere. This is also the position at which the penetrating mass shears the sheets of paper. This cylindrical shape is a friction surface as the sphere penetrates. The combined shear and friction is tentatively assumed to be expressed as S grams per cm^2. An entirely arbitrary, numerical value is assumed for S, since it is necessary on account of the manner in which the initial evaluation of the constants is made. The value of S is arbitrarily assumed to be 10 grams per cm^2. This value may appear to be small but recall that the average density of the stack of paper is 0.4609 grams per cm^3, which is to be compared to 1.0 for the density of water. In addition, the surface of the penetrating sphere is at the minimum temperature which corresponds to the melting temperature of aluminum.

Omission of u_o and u_f from the Evaluation of the Constants

In the numerical evaluation of the constants in Equation 10 by the insertion of the results of an experiment, all of the experimental data is not employed. The values that are reported from the experiment are the initial radius, r_o, of the penetrating sphere, and the final radius, 0. The density of the penetrating sphere is ρ and the average density of the stack of paper is ρ_1. The length of the path, s_f, for complete ablation is also employed. Neither Equations 10 nor 11 contain u, explicitly. This is a consequence of the relation that was developed between r and u. This relation was obtained from the simultaneous, differential equation from which the solution was eventually determined.

To obtain the final differential equation for integration, the velocity, u, was eliminated from the differential equations for integration. The velocity, u, was eliminated by using the relation that was found between u and r. As a consequence, the velocity, u_o, does not appear explicitly in either Equation 10 or 11. From a single experiment, it is almost impossible to tell much about the velocity, u. By reference to the page where the relation between u and r is obtained, it is seen that the most general solution requires a constant, C, which may multiply u. The constant could be inserted in another place in the equation, but this position is perfectly general. Until the constant is evaluated, the substitution of u for r in Equation 10 will only evaluate the constant, C. This constant may, of course, be evaluated more easily by a direct substitution in the relation between u_o and r_o. The

other apparent limit, the final radius, $r = 0$, and the apparent final velocity, $u_f = 0$, cannot be employed for the evaluation of C. The reason is that the following relation

$$\frac{1}{Cu} = \left(r \quad \frac{P_3}{P_2}\right)^3$$

is indeterminant when u is zero. Division by zero is forbidden. It is very logical that u should not be employed when $r = 0$. It is not necessary that the velocity should approach zero at the same time that the radius of the sphere becomes zero.

By reference to the equation between r and u, it is interesting to use the values for the constants, P_2 and P_3 with the ratios that are reported in Table I. With this substitution, the approximate values for C are given in Table II. The equation that relates u to r is given just above this paragraph. The following, Table II extends the results in Table I in the preceding section.

Table II

Values of C and D Calculated from Assumed Values of

C	ℓ	D
Pure Number	Pure Number	$\frac{\text{calories}}{\text{cm}^2 \text{ sec}}$
1.112	0.01	12.90
.727	0.011	103.9
.441	0.012	1516.

Evaluation of Constants with Restraints on the Variables

The next step in the study of the equations for the depth of penetration is to evaluate the constants in a way which will yield the most information on the nature of any possibly omitted factor. From this information, the initial, three differential equations may be modified, or another equation may be added. The practical evaluation of the constants will probably depend on the experiments which have already been made. Since the number of experiments for the evaluation of the constants is probably limited, the evaluation must proceed in a flexible manner while keeping the general objective in mind. The objective

is to evaluate groups of measurements in different ranges of the variables. The equation is good provided the short range particles give the same values for the constants as the long range particles.

To a limited extent, the variables r_o, u_o and s_f may be considered as the most probable variables which influence the secondary constants. The secondary, very critical constants are represented by D, ℓ and S. If this selection is found to be correct, try to vary the variables over a limited range in order to emphasize the deviations in the values of the constants. As an example, consider one of the principle variables to be the length of path, s_f. The observed lengths of path could be divided into four ranges; such as short paths, short intermediate paths, long intermediate paths and long paths. Use all values of u_o which give path lengths in one selected range. Evaluate the constants from the data for each range of s_f. If the equations were correct, the constants should be the same for each range of s_f. Then consider the same groups for the lengths of path, s_f, but select the intitial radii, r_o, of the penetrating sphere. The comparison of the difference in the results for u_o and r_o should indicate whether the relation between r and u is acceptable.

It should be emphasized that this manner of evaluating the constants is not the best way to obtain constants for the entire range of application of the basic equations, provided that the equations have been established to be correct.

Discussion of the Values of the Constants as Determined by One Experiment

There are three, grouped constants for determination, P_1, P_2, and P_3. These three constants cannot be evaluated from a single experiment, because there is not sufficient data to evaluate three constants. As indicated elsewhere, three representative ratios were determined between the important secondary constants, ℓ and D. The evaluated ratios are in the range that the final values for these two constants is expected to occur. The values of ℓ are in the range from 0.01 to 0.012. These values indicate that the thickness of the collected layer of degradated paper, ahead of the sphere, varies in thickness from 1 percent of the radius of the sphere. From the differential equation that was derived, starting with the first page on this phase, the first term on the right side in this equation is the force to accelerate this layer of paper from at rest up to the velocity of the sphere. This term appears to be relatively negligible. The really significant part of ℓ is in combination with the constant S, which represents the combined friction and shear in the second term of the differential equation.

The really critical nature of the value of ℓ appears in the term, $(P_3 + P_2 r_o)$. By reference to the definition of the constants, $P_3 = -6 \ell S$ and $P_2 = 4 \rho - 3 \ell \rho_1$. From the example for the evaluation of the constants that is given in Appendix A, the numerical values for evaluation are

$$7.5313 \times 10^9 D s_f = \frac{(P_2)^8}{(P_3 + P_2 r_o)^9} \; 0.56955 + \begin{matrix}\text{Negligible} \\ \text{term}\end{matrix}$$

$$= \frac{(P_2)^8}{(-6 \ell S + 1.052)^9} \; 0.56955$$

When S = 10 grams per cm^2 and $\ell = 0.01$, the term on the right becomes

$$= \frac{(11,062)^8}{(-0.6 + 1.052)^9} \; 0.56955$$

From the numerical values, it is apparent that the length of path s_f, in the stack of paper varies as an inverse function of ℓ.

There are three cases for which the relative values of $-6 \ell S$ and $P_2 r_o$ should be considered. In the first case, the value of $-6 \ell S$ is very much less than $P_2 r_o$. In this particular case, the penetration of the particle into the paper will be relatively small. In the second case, the term, $-6 \ell S$, is initially smaller than $P_2 r_o$ but approaches the value of $P_2 r_o$. With this range of values, the depth of penetration increases at the start and then increases more and more rapidly toward infinity as the two values approach closer and closer. Finally, the third case, the value of $-6 \ell S > P_2 r_o$. In all of the examples in this case, the length of path, s_f, is negative and this case does not represent a legitimate application for this equation.

PHASE TWO

EXPANSION OF A SPHERE OF PLASMA WITH DIFFERENT INITIAL ENERGIES

INTRODUCTION

In the introduction to this Final Report, it was indicated that progress was to be reported on four phases. Two of the four phases of the work are concerned with the problem of the penetration of a bumper plate of aluminum by a spherical stone of quartz. This phase, Phase Two, is concerned with the expansion of a sphere of plasma. The third and next phase of this report will discuss the progress on the early stages of obtaining a computer program for the penetration of a sphere of rock through a thin plate of aluminum. As the penetration by the rock proceeds, a shock front compresses the volumes of aluminum and of rock in the curvilinear squares by different amounts. Every shock compression increases the entropy of the compressed material. In the most general case, the expansion after compression is along an isentrope, i.e. along a line of constant entropy. This general case would require some energy to be dissipated during the expansion. Metals that are shock compressed, usually are considered to expand along an adiabat with no dissipation of energy. This means that after adiabatic expansion, from shock compression, the metal retains a considerable amount of internal energy in the form of heat. This brief statement is an oversimplification of several papers, such as the paper by G. E. Duvall and G. R. Fowles,[1] and of other publications that are cited in this particular paper.

The heat that is retained by the metal after shock compression and adiabatic expansion to atmospheric pressure may range from simple heating of the metal, to producing molten metal, to producing a plasma. The total amount of heat is dependent on the magnitude of the initial compression. The thesis by Hardage estimates that shock compression to 37-1/2 kilobars will result in leaving aluminum molten after it has expanded, adiabatically to atmospheric pressure. Shock compression into the megabar range converts the aluminum metal into an aluminum plasma. In the penetration of the bumper plate, the energy content is divided into kinetic energy and into internal energy for each of the mesh volumes. As is customary with computer solutions, the solution is for finite differences. This requires all space to be divided into cubes, or regularly shaped volumes for cartesian coordi-

nates. When spherical coordinates are employed, as in this problem, the volumes for consideration are curvilinear cubes. For each of these cubes, the kinetic and the internal energy are given in the computer print-out. Since the expansion is adiabatic, the internal energy of the curvilinear cube should not change during the expansion. This internal energy may be employed at any time to identify the end product as a hot metal, a molten metal, or as a metallic plasma. As a consequence, a shift from the Mie-Grünesen equation of state to the plasma equation of state may be made at any time during the expansion.

After a one by one change of the curvilinear cubes from compressed metal to compressed plasma, the expelled material from the impact zone must continue to expand. More specifically, the material that is expelled by the rock penetrating the thin plate must expand as a mixture of aluminum plasma, rock plasma, molten aluminum, molten rock, pieces of hot aluminum metal and perhaps pieces of hot rock. The plasma portion of the expelled material will expand to interlace the entire mixture.

For this particular phase of the problem for study, the preceding discussion does not need to be followed farther from a general viewpoint. If an aluminum plasma is produced, it must be shown that this group has the capability to consider the expansion from a dense plasma to a very tenuous plasma. The initial work on the expansion of a plasma by a member of this group was by R. E. Bruce. The work on the expansion of a sphere of plasma was the subject of the Ph.D. thesis by Dr. Bruce. This ex-student from this group is presently an Associate Professor of Physics at the University of Texas at El Paso. The thesis by Dr. Bruce has been distributed to the mailing list on this contract, as well as is presently recalled by the author. For this reason, reference is frequently made to his thesis, instead of to the original references. There are several parts of Dr. Bruce's thesis which were in error. In particular, there are serious errors in the curves in the original thesis and in the manner in which the solution behaved near to the vertical axis along a diameter of the sphere of rock. Dr. Bruce was paid, as a consultant, to come to UAH for the purpose of teaching a present student to run his program and to rerun the programs in the original thesis. In order for the results to be more reliable, the curves in the remainder of this section are from the new runs by Dr. R. E. Bruce.

GENERAL BASIS FOR A CALCULATION OF THE EXPANSION OF A SPHERE OF PLASMA

For an understanding of the method of calculation, reference is made to Chapter V in Bruce's thesis. (pp. 77- 89) There is nothing particularly unique about the formulation of the equations. Scaler pressures are employed instead of tensor pressures. As is usual for a scaler pressure, an equation of state was obtained. This equation of state is unique as far as references were concerned at the time that the thesis was written. At the first of this calendar year, Bruce informed me that a similar equation of state with this elaboration has not yet been published in the literature that he had investigated. The evaluation of the accompanying curves in this phase of this report requires an understanding of the equation of state so this subject is discussed in the next section. Before proceeding with a discussion of the equation of state, two other subjects require some discussion. One subject is concerned with the effect of microfields and the other is the equation of state at extremely high densities.

Microfields in Dense Plasmas

A discussion of the microfields in the plasma is essential for understanding the method of procedure. The subject of microfields will recur in this report, so a quick introduction is given here. In the plasma, there are ions of various specie which are intermixed with sufficient electrons to give a neutral plasma. As an example, a particularly hot plasma may have Al^{+2}, Al^{+3}, Al^{+4} ions in a proportion that may be predicted from their relative ionization potentials in the plasma and from the application of Boltzmann's law. These ions and the matching electron cloud for neutrality produce microfields and these microfields lower the ionization potential for the production of ions. It is immediately apparent, that increases in the density of the ions and their accompanying electrons will increase the magnitude of the microfields and this further lowers the ionization potential to produce the ions.

The lowering of the ionization potential by the microfields will be considered again under the discussion of the formulation of the equation of state for the plasma.

The calculation of the number of each specie of ions would require a total of 16 simultaneous equations instead of five and probably from five to nine times the computation costs. In order to avoid this additional cost, an average ionization is calculated. This is a peculiar type of average that will give roughly the same characteristics in the plasma as the true distribution of ions would give. This average number of ions is the ordinate for one of the curves in most of the graphs that represent the expansion of the plasma.

Equation of State Employed for Subsequent Calculations

In many studies of plasmas, the equation of state is taken as the perfect gas law. The perfect gas law considers the atoms to exert no forces on each other, except by collisions. In other words, the atoms behave roughly like a cloud of ping pong balls; i.e. there is no interaction except for completely elastic forces which are active only when the balls collide with each other. For a complete description of all of the terms in the equation of state, the reader is referred to Bruce's thesis. For the present discussion, the equation is presented and the nature of each term is identified in very general terms.

In the presented equation of state, there are terms which affect the plasma by different amounts in different circumstances, and some terms may often be omitted. The general form of the equation is given in terms of the internal energy which is expressed in terms of the temperature and the density; i.e. the equation of state has the form $E_{TOT} = E(\rho, T)$. In every case, the plasma is considered to be formed of aluminum atoms, ions and electrons. It is to be recalled that the plasma is always considered to be neutral; i.e. the plasma has no net, average charge. There is a minor exception to this general statement, there may be local charges that build up in oscillations between the positive ions and an oscillating electron cloud. These oscillations constitute one term in the equation of state. After this preliminary introduction, the general form of the equation of state is given by the following relation:

$$E_{TOT} = E_{ID} + E_{ION} + E_{EXC} + E_{IN} + E_{DEG} + E_{RAD} + E_{OSC}$$

In this relation, E_{TOT} is the total energy in the plasma. Each term will be discussed in some detail, but only in sufficient detail to identify it. There is not sufficient detail to perform the calculation for each term.

The first component of the energy is E_{ID} where the subscript is an abbreviation for ideal. This term represents the kinetic energy in the perfect gas law. This energy is given by the relation

$$E_{ID} = \frac{3}{2} kT \left(C_e + \sum_i C_i \right)$$

where C_e represents the number of electrons and C_i represents the number of ions of each specie, i. The ions include C_o which is the neutral aluminum atom. It is to be observed that each electron and each atom has the same average energy. This relation is immediately recognized as

$$\frac{1}{2} m v^2 = \frac{3}{2} kT.$$

The second term is deisgnated as E_{ION}. This is the energy that is required to ionize the different specie to form the plasma and this energy must be lowered to compensate for the effect of the microfields. Formally, the energy may be indicated in the following manner

$$E_{ION} = \sum_i C_i \left(\sum_j^{j-1} I_j \right) = C_2 I_1 + C_3 (I_1 + I_2) + \ldots\ldots$$

There is difficulty in evaluating this relation when it is expressed in this particular form. The average ionization is calculated by a redistribution of the energy between all of the different available forms of energy that are expressed in the equation of state. This requires reiterative calculations for the solution to converge on the proper number of ions with the necessary number of electrons to obtain a neutral plasma. Designate the energy that is found by this calculation to be I. Then the quantity, E_{ION} is given by

$$E_{ION} = I - \Delta I$$

where ΔI is the Ecker and Kröll correction for the effect of the microfields on lowering the ionization potential. The technique for obtaining the average ionization and the lowering of the ionization potential by the Ecker and Kröll method is outlined in Bruce's

thesis. It should be mentioned that Bruce says that he finds it necessary to recalculate the convergence on every third cycle through the program. The last equation above is given in order to emphasize the nature of the solution that is obtained and is not a description of the mathematical steps that are employed.

The third term on the right is E_{EXC} and this term represents the excitation energy that is in the equation of state. Every available energy will have electrons in it according to the maximum number of electrons in the plasma and the possible levels in the ionized atoms and the degree to which the excited levels are filled. The excitation levels are filled according to their energy by the Boltzmann relation. A general, analytical representation is

$$E_{EXC} = \sum_i \left(\frac{C_i}{Z_i}\right)\left[\sum_j^{j_{max}} E_{ij} \cdot g_{ij} \exp\left(-\frac{E_{ij}}{kT}\right)\right]$$

The term on the extreme right is the Boltzman relation for filling the g excitation levels in the ions. There is a difficulty with this relation as solid density is approached, or as the density of ionization becomes very high. The microfields, in either case, exert sufficient forces on the ions to require quantization of the energy levels. This requires the application of the Pauli exclusion principle to limit the possible number of electrons in the excited states. This quantization is important and is mentioned later in this report.

The fourth term is designated as E_{IN}. This is an evaluation of the energy that arises from the interaction of the microfields between the different particles in the plasma. The specific name for the method of calculation is the configuration integral.

In more familiar terminology, it is referred to as the calculation of the cluster integrals for all particles, pair-wise. This is often mentioned in the literature as the two-body cluster integrals. The interaction energy is calculated for all particles, considered two at a time. The correction to the equation of state is particularly important in dense plasmas but trailed off to a negligible correction at densities from 10^{-3} to 10^{-4} times the density of solid aluminum. It decreases with the density until the correction becomes negligible at the above limiting densities and the equation of state converges on the prediction of the perfect gas law.

The fifth term for the correction to the equation of state is E_{DEG}, where the subscript refers to the degeneracy. This correction comes from the work of Wigner and is described by Bruce. The term varies as the order in the plasma decreases from the density of a solid to the density of a rarified gas.

The sixth term is E_{RAD} for the radiation energy that is generated and is probably not trapped in the hot plasma. For plasmas in the temperature and density range which are of interest for this project, this term is neglected. By neglecting the energy in the radiation, the energy in the sphere remains in the sphere. If the energy were allowed to radiate, there would be a very difficult correction to the entire system of equations which is not of sufficient magnitude to be significant for the relatively low temperature and short duration of the plasmas for which these calculations are applicable. As an example, the expansion could not be adiabatic if the radiation should escape.

The seventh and last term is E_{OSC}. This term represents the energy in the self-excited oscillations of the electron cloud relative to the ions in the plasma. This is a difficult term to evaluate so a partial correction is employed at this time. The correction is not large and additional corrections may be required for other plasmas.

Limitation on this Equation of State

The equation of state that has been presented is quite accurate until the density approaches solid state. The nature of the deviation is shown by the curves in Figure 2. These curves show the electron density as a function of the density in grams per cm^3 for a constant energy added to the gas. For a perfect gas, the density of ionization of hydrogen gas may be calculated from the perfect gas law with the aid of Saha's equation when the added energy is known. In the cases to be considered at this time, the added energy is either 2 eV per atom, or 5 eV per atom. The lower curve in each of the two graphs in Figure 2 shows the electron density as a function of the total density for 2 eV and 5 eV. according to the label on the graph. As the density increases toward the left in the graphs, the density of electrons continues to increase with the mass density.

As a consequence of the lowering of the ionization potential by the increased effect of the microfields, the density of electrons increase faster with the mass density

than predicted by the perfect gas law in combination with Saha's equation. This is illustrated by the curves in Figure 2. The lower curve is the perfect gas law combined with the Saha equation. The middle curve is for the lowering of the ionization potential that is predicted by the Ecker and Kroll relation. In every case, the gas is hydrogen.

For hydrogen gas, alone, there is a third analytical method to check the magnitude of the correction and this method is precise, except the solution depends on the amount of energy in the other terms in the equation of state. The density of ionization may be calculated with the Schroedinger equation by employing the Yukawa potential. The Yukawa potential is for a central charge that is partially shielded, in this case, by electrons. The calculated check on the ionization is the upper curve in the two graphs in Figure 2. From this check calculation, it would appear that the Ecker and Kroll relation does not predict enough ionization. Another sink is known for the energy and it has been investigated.

The agreement between the top two curves is only fair and the agreement should be better. This conclusion follows from the evidence that the Schroedinger equation with the Yukawa potential gives an electron density that is systematically too high. The source of the error appears to be explainable. The interaction energy, E_{IN}, exists in the plasma to which the Schroedinger calculation is applied, but no correction for it has been included in the data that is plotted. When the correction for the two body interaction is included, it gives a lower electron density than the Ecker and Kroll result. At the same time, the curve with only the Ecker and Kroll relation should be slightly lower because of the three body, cluster integral correction on the energy content. The three body cluster integral is mentioned below. It is to be emphasized that the actual correction and the added corrections have not been calculated although only arithmetic operations are necessary.

In the calculation of E_{IN}, the interaction was found on the basis of cluster integral calculations on the so-called two body basis. An investigation showed that the inclusion of three body forces would reduce E_{IN}. It was also shown that four body interaction would be exceedingly low and would have a negligible effect. In a M.S. thesis for the Mathematics Department at Oklahoma State University, Mr. H. A. Reeder calculated the three

Figure 2. Equation of state plotted for hydrogen as a log-log relation between the electron density vs the mass density for a total average energy of 2 eV per atom in the upper graph and 5 eV per atom in the lower graph. At the upper left in both graphs, the curve splits into three parts to represent the effect of lowering the ionization potential of hydrogen (a) the upper branch represents hydrogen as calculated by the Schroedinger equation with the Yukawa potential, (b) the intermediate branch by the Ecker and Kroll relation and (c) the lower branch contains no correction and comes from the perfect gas law and the Saha equation.

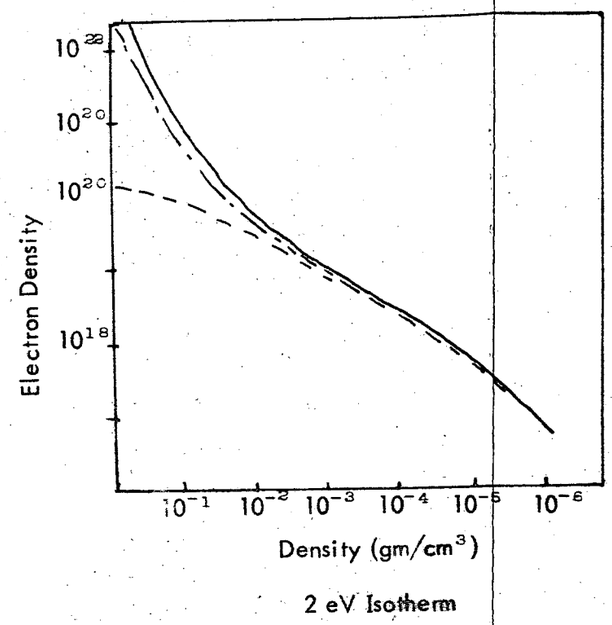

2 eV Isotherm

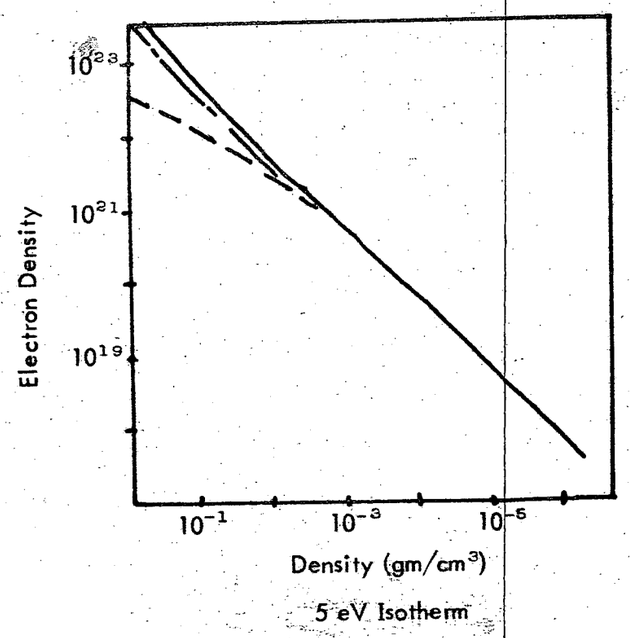

5 eV Isotherm

body cluster integral. The three body cluster integrals were for hydrogen and Reeder omitted the terms in the three body cluster integrals that were not symmetrical. For ionized hydrogen, these unsymmetrical terms could not exist. His results are given for an added energy of 5 eV. There is a graph from his work which is designated as Figure 3 in this report. The upper dotted curve is Bruce's two body calculations, the dahsed, intermediate curve is Reeder's calculation with both the two body and the three body terms. The lower curve is the calculation from the perfect gas law and Saha's equation.

PRESENTATION OF RESULTS

With the complex equation of state that has been derived, the expansion of a sphere of plasma is very different from an expansion with the perfect gas law as the equation of state. The principle effect from the extended equation of state is a consequence of the term for lowering the ionization potential and the term for the internal energy in the microfields, E_{IN}. Before presenting the graphs, a few general comments are made on the overall object of the computation for the expansion and on the general assumptions for the computation.

General Statement of the Problem

The computer calculations are to obtain the solution to a "gendanken" experiment. In this experiment, a sphere of solid aluminum is considered. At time, $t = 0$, each atom in the sphere receives the same amount of energy. In this report, there are three computer solutions with the added energy per atom at 44.45 eV, 20.8 eV and 7.136 eV, respectively. The solution is calculated in terms of dimensionless variables. In the presented graphs from the solution, the dimensionless variables have been converted to dimensions. The initial radius of the sphere is about 4×10^{-3} cm. The abscissa of the graphs is dimensioned in terms of this starting radius and the graphs show the growth of the radius as the plasma expands into a vacuum.

In the preceding discussion, the conditions for the solution are discussed in considerable detail. One very basic condition has been assumed without a specific statement of the postulate up to this time. This condition requires that equilibrium must exist

Figure 3. A log-log plot of electron density against the mass density for a hydrogen plasma. As in Figure 2, the curve divides into three branches in the upper left corner of the graph. These three branches show the effect of increasing the accuracy of the equation of state by means of a more precise calculation of E_{IN} in the equation of state. (a) The upper branch shows the effect of the two body cluster integrals on the density of electrons. (b) The intermediate branch of the three branches shows the effect of two body cluster integrals plus three body, symmetrical components only, on the density of electrons. This is the most accurate curve in the group. (c) The lower branch in the upper left is for the perfect gas law and the Saha equation with no correction for the interaction fields.

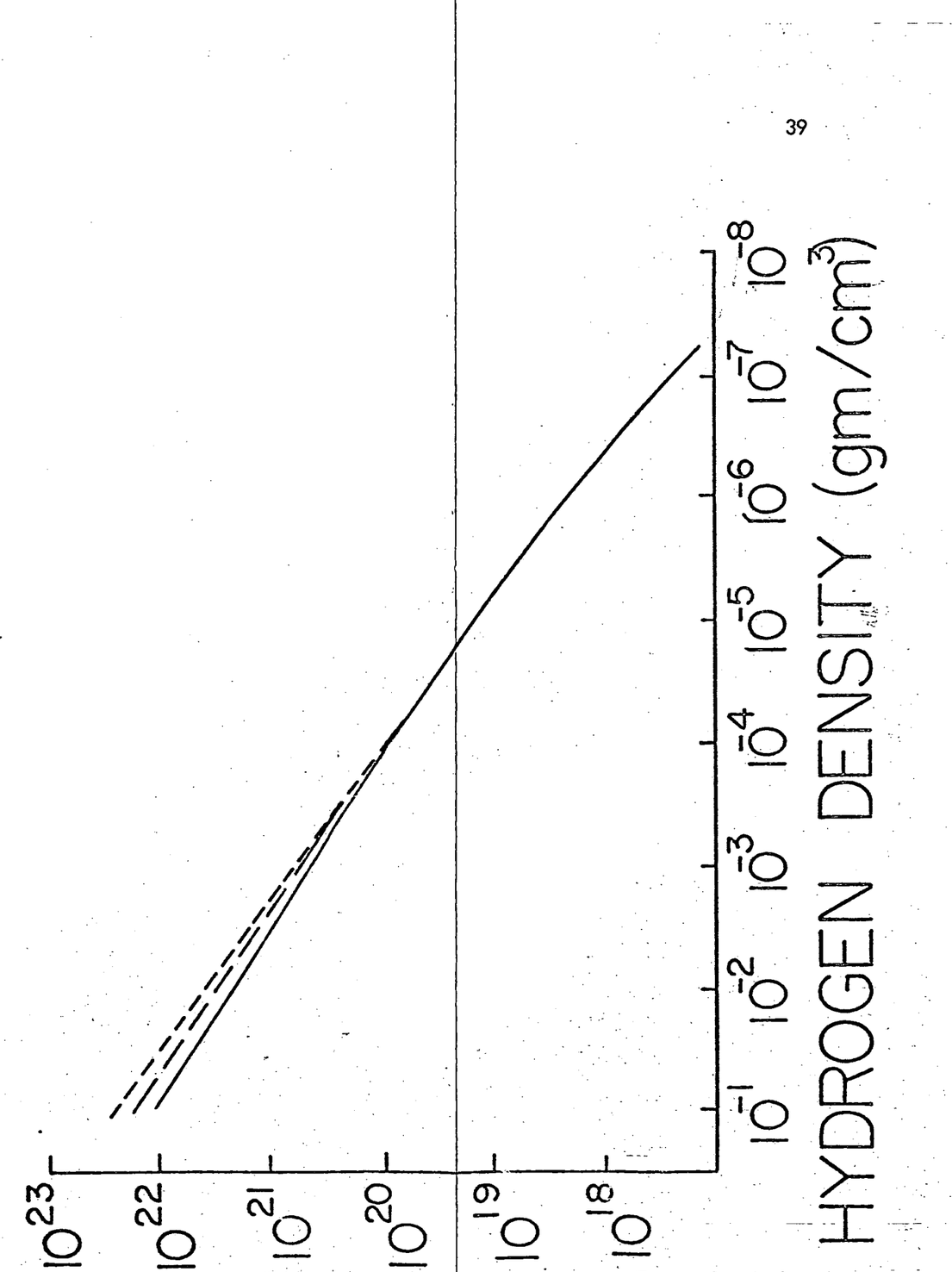

at all times. In particular, this requires that ions and excited states exchange energy instantly. This requirement cannot possibly be correct. The mean life of an Al^{+1} ion is about 12×10^{-9} seconds. This value was read from a curve that was part of the Ed.D thesis of Dr. Vernon D. Brown. Brown is presently an Associate Professor at Memphis State University. The mean life of aluminum ions with a higher state of ionization, such as Al^{+3}, Al^{+4} and Al^{+5}, is much shorter. This conclusion of a shorter mean life comes directly from the application of the uncertainty principle. The first expansion with an initial energy of 44.45 eV per atom is followed for a total time of 5.861×10^{-9} seconds. Ions of Al^{+5} and Al^{+4} would certainly radiate in this time interval but not Al^{+1}. A correction for the mean life will certainly change the form of the solution, but the correction is very involved. It is desired, therefore, to have the solution for instantaneous equilibrium.

In the solutions that are presented, the energies are rather large. The reason for selecting these energies is to avoid, as much as feasible, an expansion in a region with densities near to solid state density. The multi-corrected equation of state does not have a good correction for that region. A better equation of state is available from the work of Larry J. Peery. Peery obtained the correction in his Ph.D. thesis while working with this group. Peery is presently a Professor at Central Methodist College at Fayette, Mo. His improvement in the equation of state consisted of a careful interpolation from (a) the accurate equation at mass densities for 10^{-2} to 10^{-3} grams per cm^3 to (b) the density of solid aluminum.

Expansion of a Plasma with an Initial Energy of 44.5 eV per Atom

The first graph of the expansion is for an instant of time that is very soon after the expansion starts. As shown in Figure 4, the exact time is 0.6845×10^{-9} seconds after the start of the expansion. The density is constant at the origin and is the initial density; i.e., the density of solid aluminum. The average ionization potential decreases in two steps with a break in the slope between the two rates. The break is near an average ionization potential of about 3 eV. There is a corresponding small hump in the density at the same radius. This hump is slightly masked in the reproduction. The discontinuity at about 3 eV indicates that this is probably an ionization potential, or perhaps an

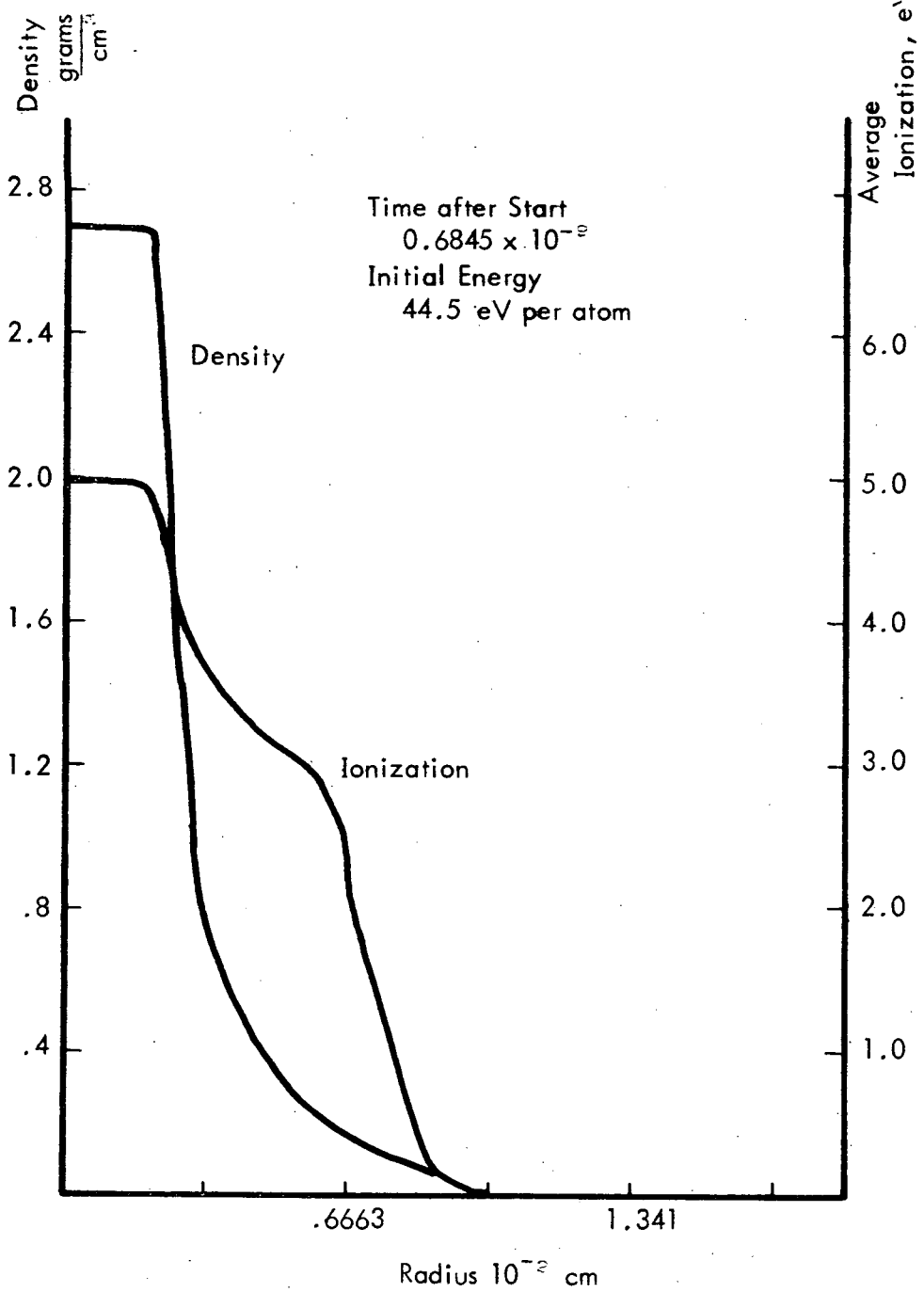

Figure 4. Density and Average Ionization Variation with the Radius (44.5 - .68)

excited state in the aluminum plasma. If this explanation is correct, more breaks should be observed in the graphs for other time intervals.

The second graph in Figure 5 shows the expansion at a later time, 1.372×10^{-9} seconds. The peak density has decreased by almost a factor of 10 from the density in the preceding graph. The average ionization potential shows two peaks, there is one at about 3 eV, which appears to be the same one as in the preceding graph, Figure 4. There is a second break in the slope of the average ionization potential at a little over 1 eV. These breaks indicate that the conditions at the two radii are such as to emphasize an ionization potential, or an excitation level. Recall that the ionization potentials are finite and are separated. The Boltzmann relation is exponential so the curve is not symmetrical between the levels.

As time continues, the expansion continues but assumes a different form. The expansion at 2.059×10^{-9} seconds is shown in Figure 6. The density has dropped almost another factor of 10 from the preceding figure. The most startling difference is that the density decreases in the center of the sphere and the density is starting to form a cold shell of plasma outside the hot core. The hot and cold plasmas are identified by the average ionization. If the average ionization is of the order of 4.5 eV, the plasma must have a high internal energy. Conversely, if the average ionization potential is nearly zero, there is not sufficient internal energy to be hot. There are humps in the average ionization which correspond to average ionization, or excitation potentials such as were identified in the preceding graphs.

As the expansion continues, the formation of a hot, low density core becomes more clearly established. This hot core is surrounded by a cold, high density shell. This is demonstrated by the curves in Figure 7 which is for a time of 2.746×10^{-9} seconds after the expansion starts. A closer inspection of the curves in this figure show that the average ionization at the center of the sphere has increased over the value at the center of the sphere in the preceding graph, Figure 6. This indicates that a hot core forms, and in additon the average ionization, or the effective temperature of the core also increases.

In the last of the expansion curves for an initial energy of 44.45 eV, the hot core and the cold shell have fully formed. This expansion, at 5.861×10^{-9} seconds after the start is presented in Figure 8. The average ionization in the hot core is even higher

Figure 5. Density and Average Ionization Variation with the Radius (44.5 - 1.3)

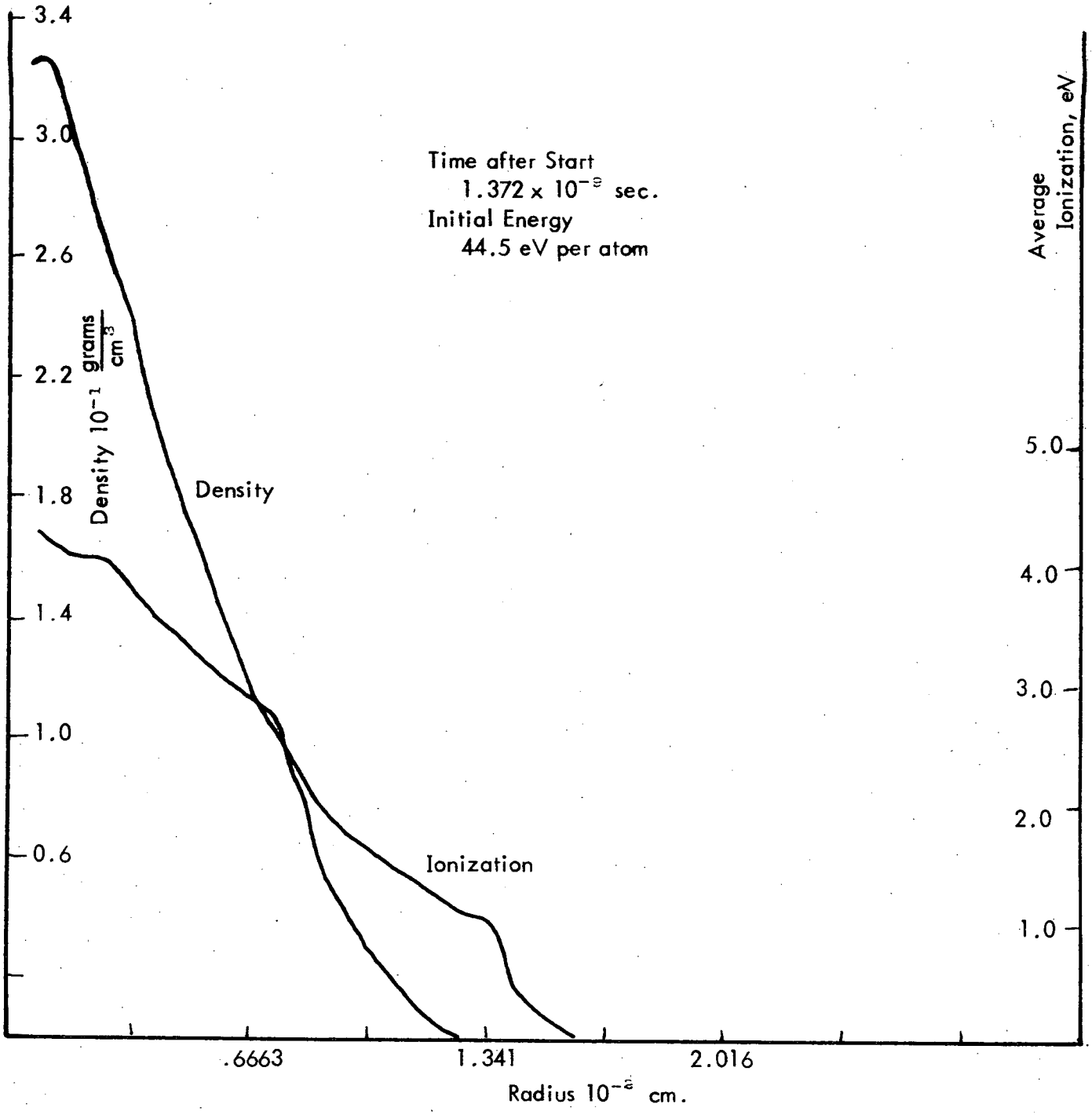

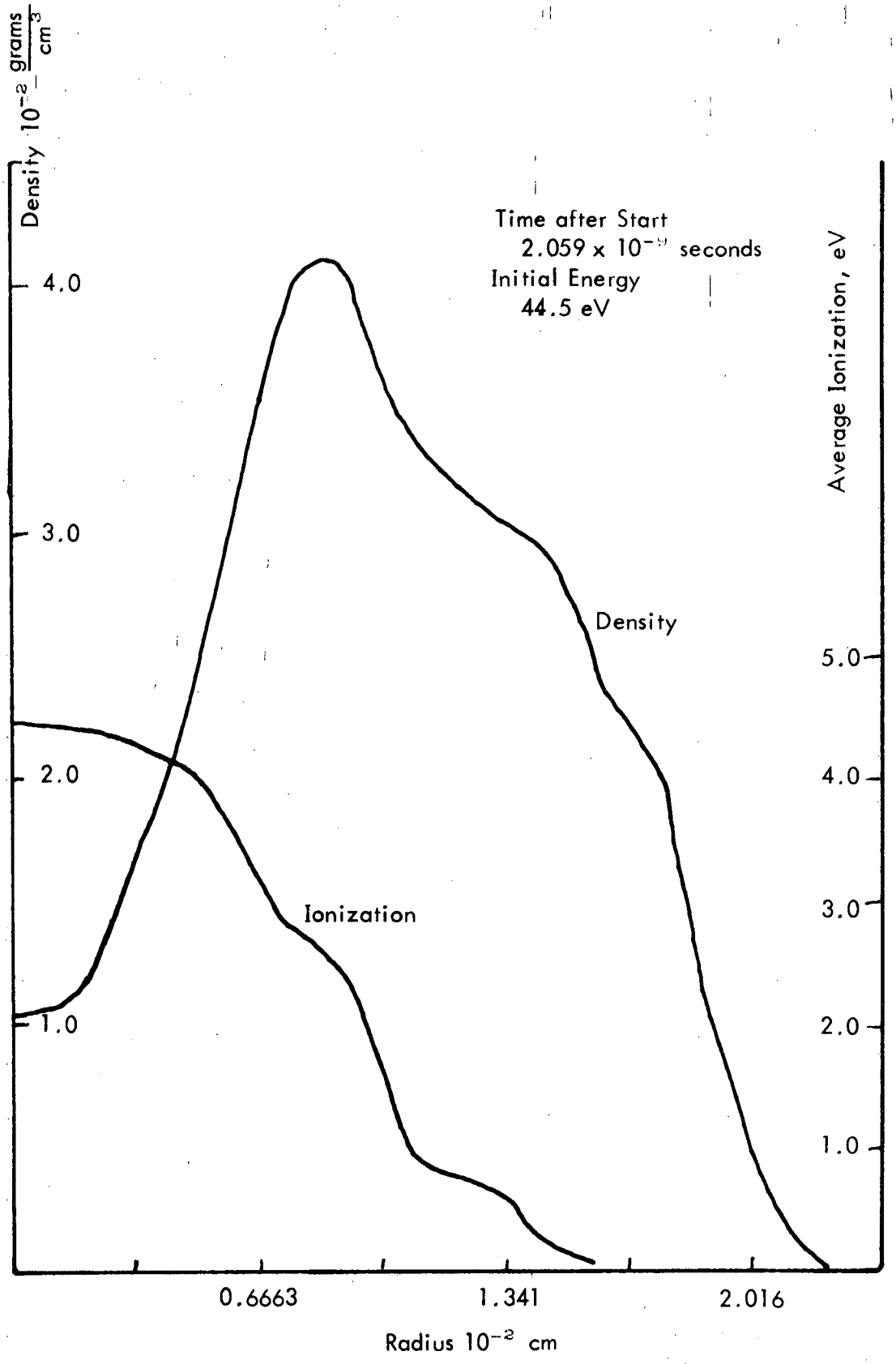

Figure 6. Density and Average Ionization Variation with the Radius (44.5 - 2.0)

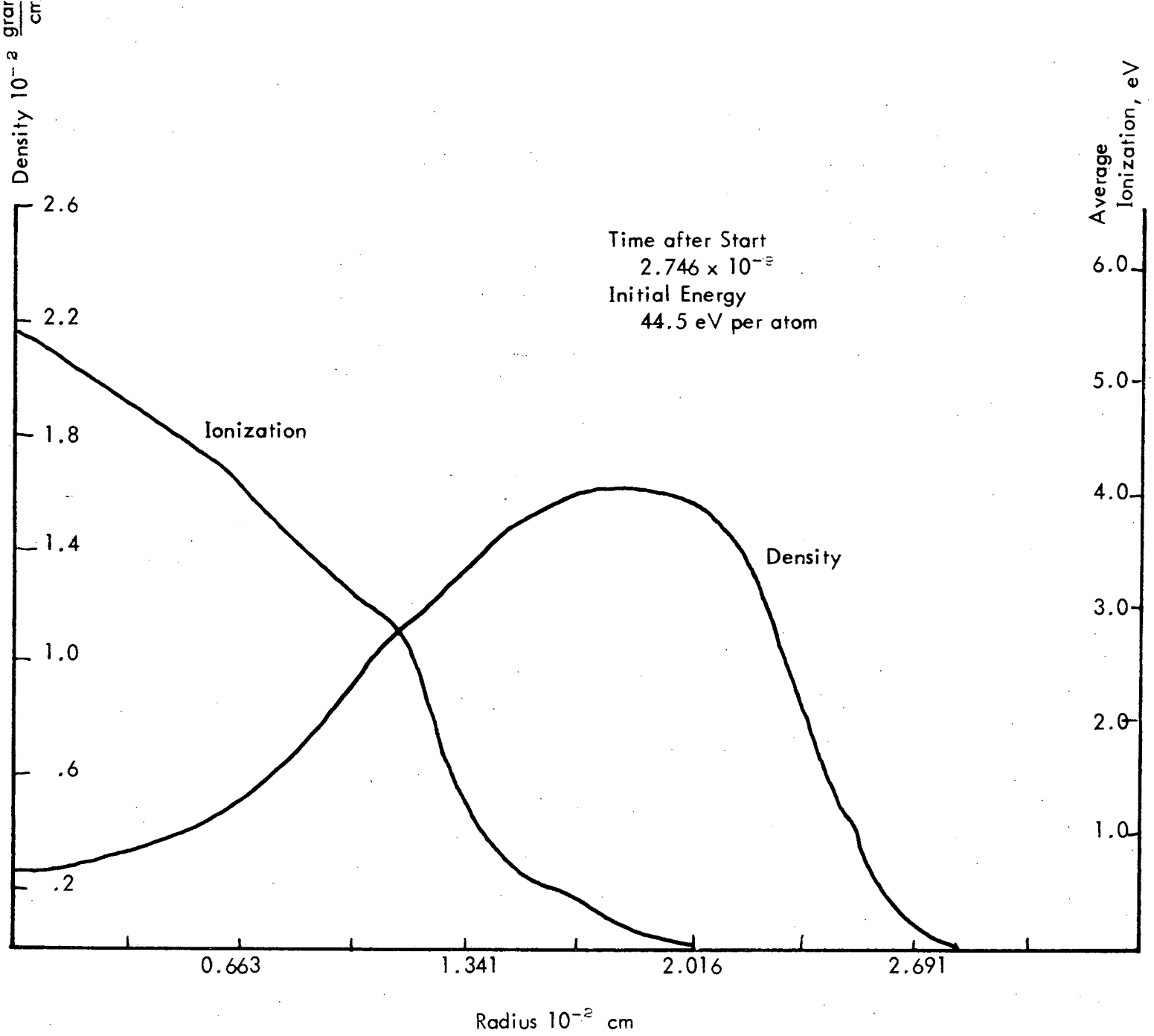

Figure 7. Density and Average Ionization Variation with the Radius (44.5 - 2.7)

than the initial average ionization. The initial average ionization from the computer print-out is 5.011 eV. In the hot core in Figure 8, the average ionization is 5.550 eV. In this and in the preceding graphs, the average ionization has been used as an indication of the temperature. In this graph, the temperature is plotted. The temperature is the curve that plunges off the bottom of the page in the center of the plot. All of the ordinates in this graph are linear and all of the curves except the temperature have zero at the bottom of the graph. In order to determine the extent of the decrease in temperature, a plot of the temperature and the pressure are shown in Figure 9. This data is for the same instant of time as Figure 8. The ordinates for both the temperature and the pressure are logrithmic. It is to be observed that the temperature has decreased over three decades at a radius that corresponds to the peak of the density in the cold shell.

A short summary is presented of the most obvious facts that are disclosed by the graphs for the expansion of the very high energy plasma.

a. The expansion forms a hot core that is surrounded by a cold shell.

b. Humps on the curves for the average ionization indicate the existence of the levels for ionization, and/or excited states in the plasma. This information was given to the computer by the E_{EXC} term in the equation of state.

c. The cold shell is really rather cold according to the computer print-out.

The less obvious facts will be presented after comments are made on the remainder of the curves. There is one subject that should be mentioned. The hot core with the cold shell is an intrincically unstable condition. By light emission during the formation of the cold shell, its formation has been confirmed. Before the shell has the density range in Figure 8, the shell becomes unstable and breaks up to reveal the hot core. The break-up has been confirmed by the intensity of the emitted light.

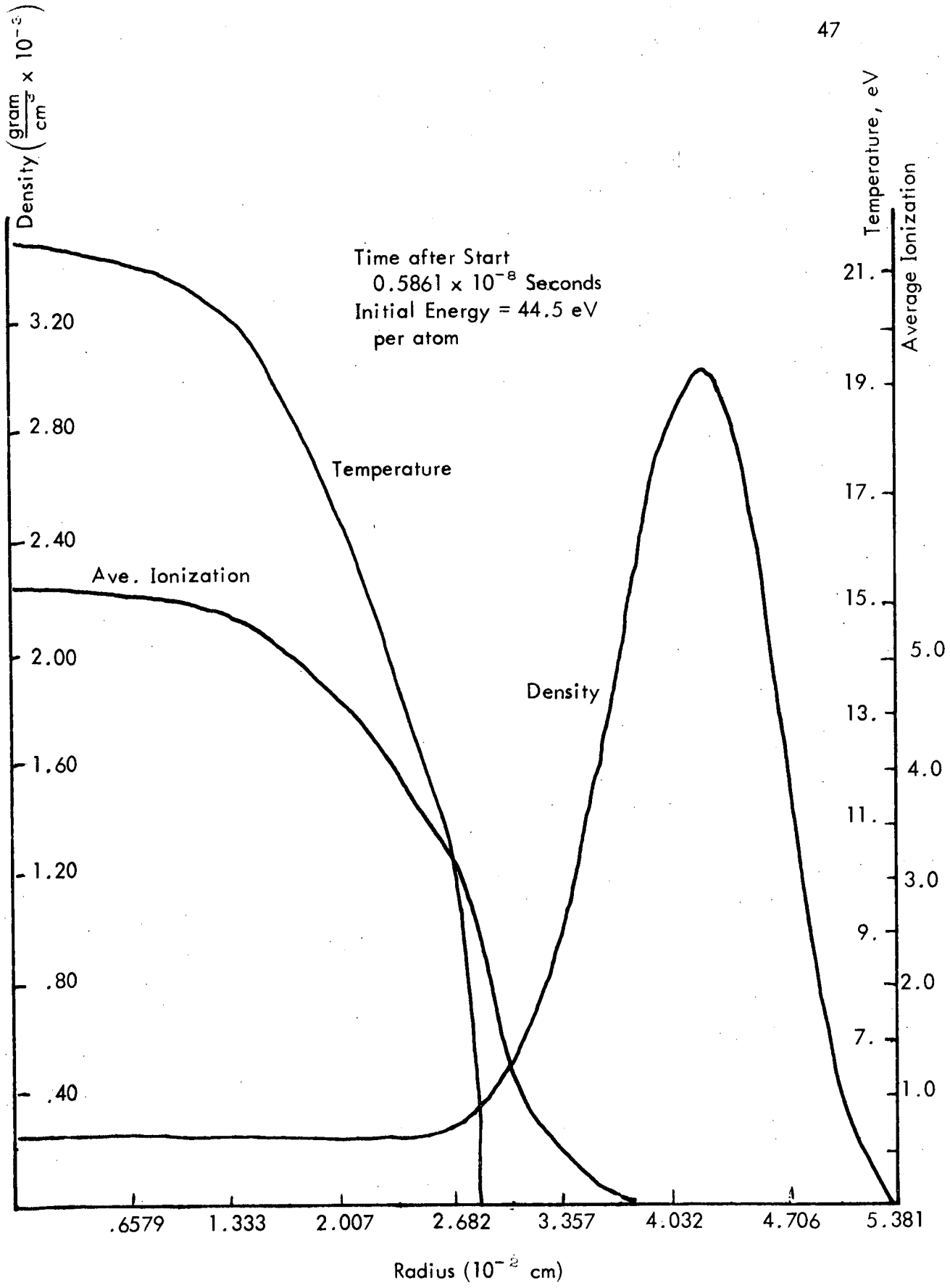

Figure 8. Density and Average Ionization Variation with the Radius.

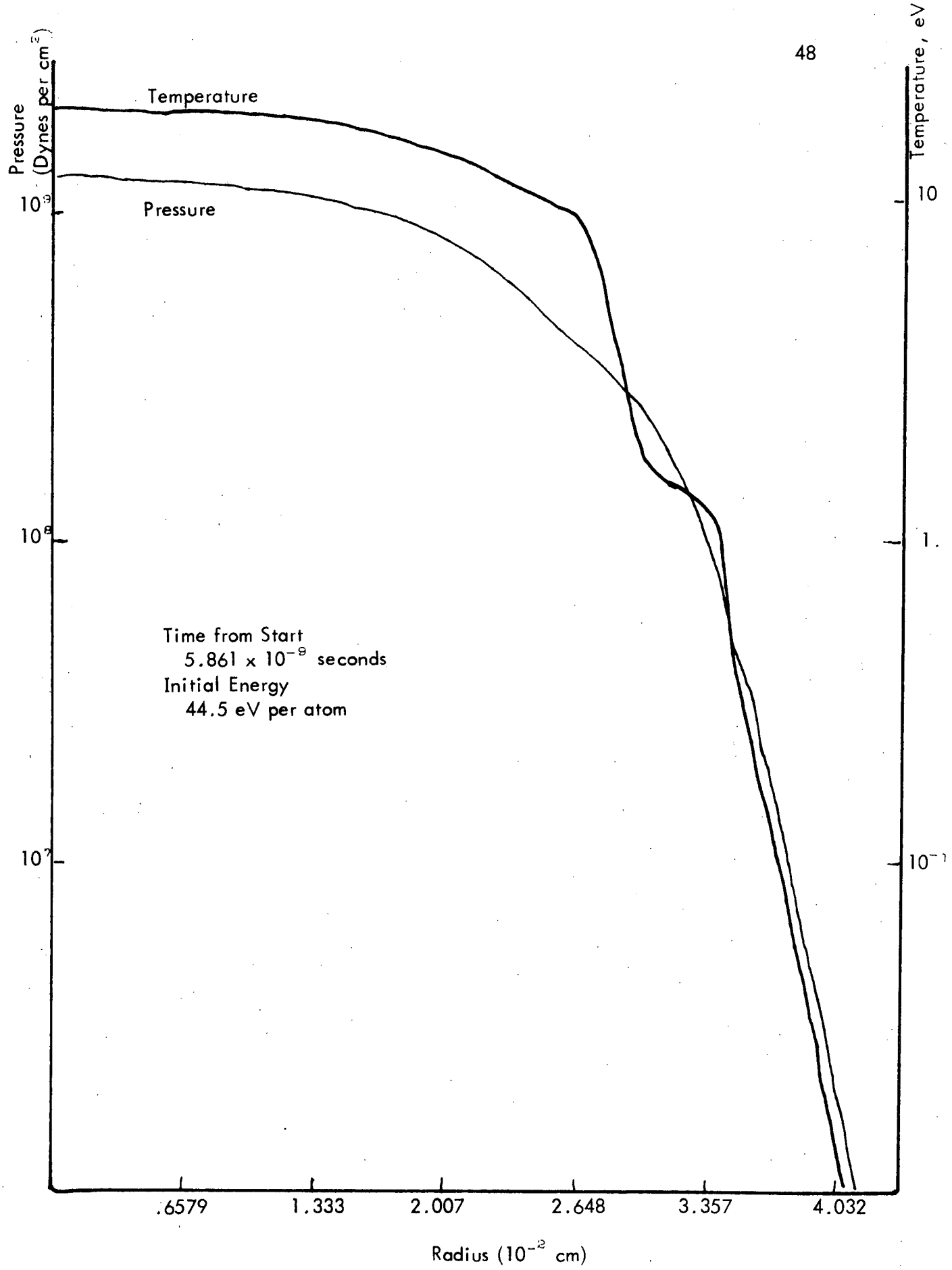

Figure 9. Semilogrithmic Scale of Temperature and Pressure Variation with the Radius.

Expansion of a Plasma with an Initial Energy of 20.8 eV per Atom

For comparison with the description of the expansion of a sphere of plasma with very high energy content, some graphs are presented to show the expansion of a plasma with less than half of the high energy in the first expansion. The actual energy contents are 20.8 eV per atom in contrast to 44.45 eV per atom. The same number of atoms are involved in each case.

The first graph for the expansion is given for a time of 1.108×10^{-9} seconds after the start of the expansion. The curves in this graph, Figure 10, are for the lower energy, 20.8 eV per atom. They are to be compared with the high energy graphs that are presented in Figure 4 and Figure 5 which are for 0.6845×10^{-9} seconds and 1.372×10^{-9} seconds, respectively, after the expansion started. The curves for the lower temperature, in Figure 10, show a slower expansion of the high density material in the core. This would be expected. The breaks in the curves for the average ionization are more pronounced than at the higher temperatures. A break in the average ionization still occurs near the average value of 3 eV. The exact value fluctuates about the 3 eV level. This is to be anticipated and depends on the density, the temperature, the location of excitation levels and other factors.

As the expansion continues, the density still corresponds to the initial solid state density although the expansion started 2.261×10^{-9} seconds before the curves in Figure 11. The "knees" in the average ionization curve are more pronounced than ever.

As the expansion continues, the start of the formation of the hot, low density core is well defined in Figure 12. This graph illustrates the state of the expansion and of the average ionization after 3.413×10^{-9} seconds. There is nothing particularly new with respect to the results in other graphs.

The hot, low density core is well defined in the next graph. The set of curves in Figure 13 were obtained 4.565×10^{-9} seconds after the start of the expansion. The curve for the average ionization looks rather distorted from the presence of strongly emphasized ionization and/or excitation levels near 3.0 eV and below 1.0 eV. This is approximately the relative distribution between hot core and cold shell at which the combination becomes so unstable in the practical case that it breaks up, or more probably, it just decomposes. This is a highly arbitrary conclusion, although there are a few threads of

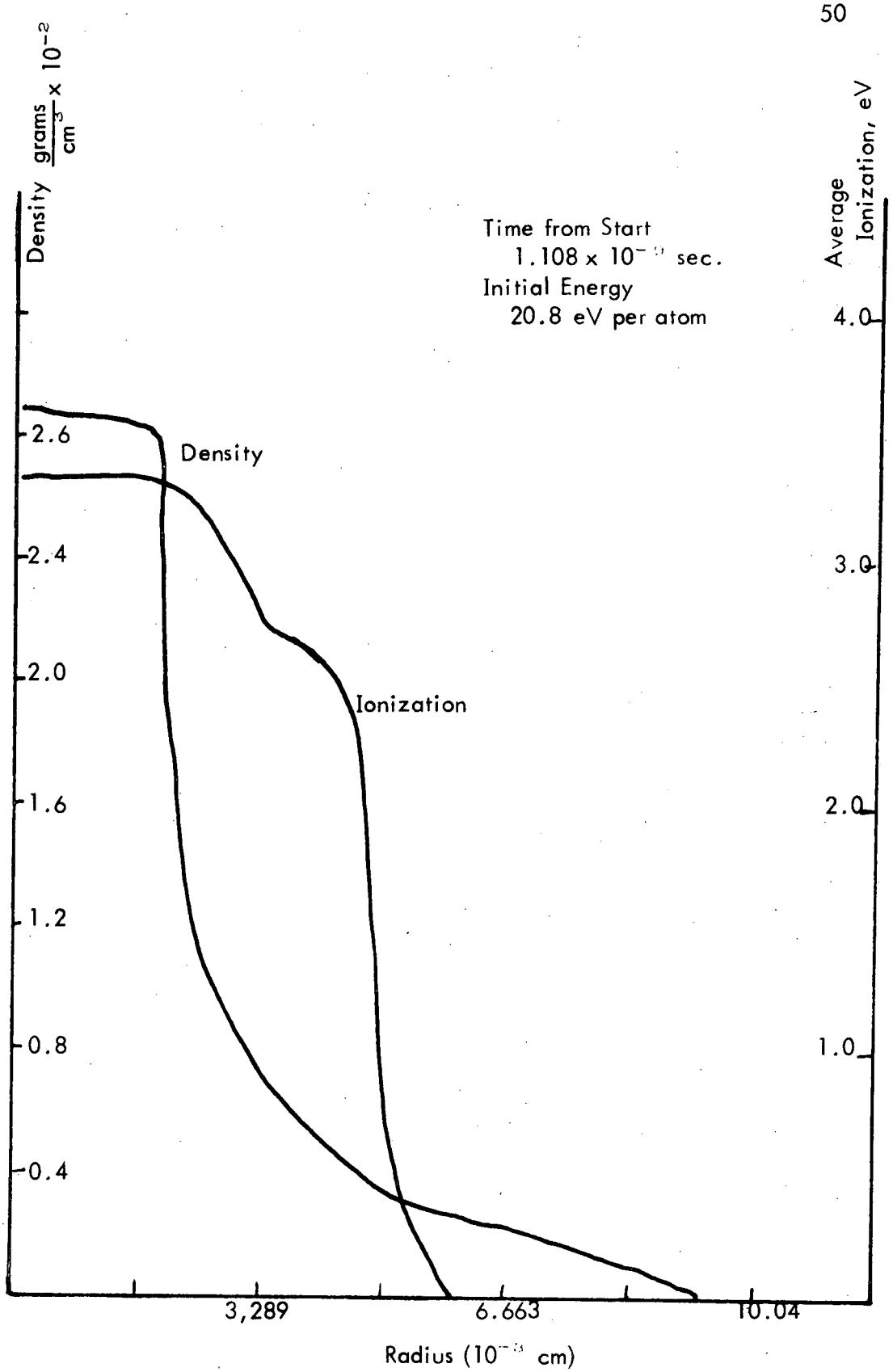

Figure 10. Density and Average Ionization Variation with Temperature (20.8 - 1.1)

Figure 11. Density and Average Ionization Variation with the Radius (20.8 - 2.26)

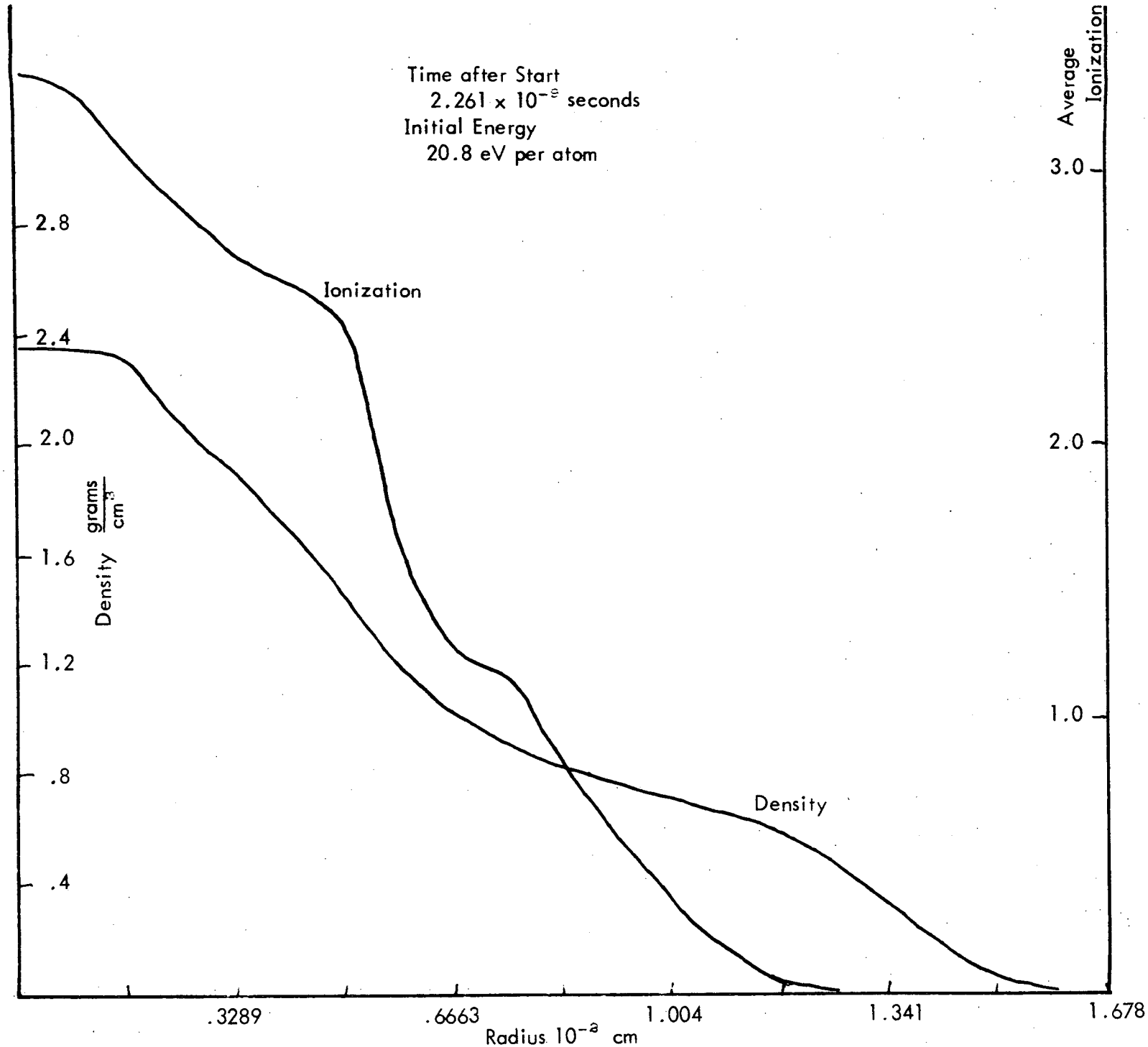

Figure 12. Density and Average Ionization Variation with Radius (20.8 - 3.4)

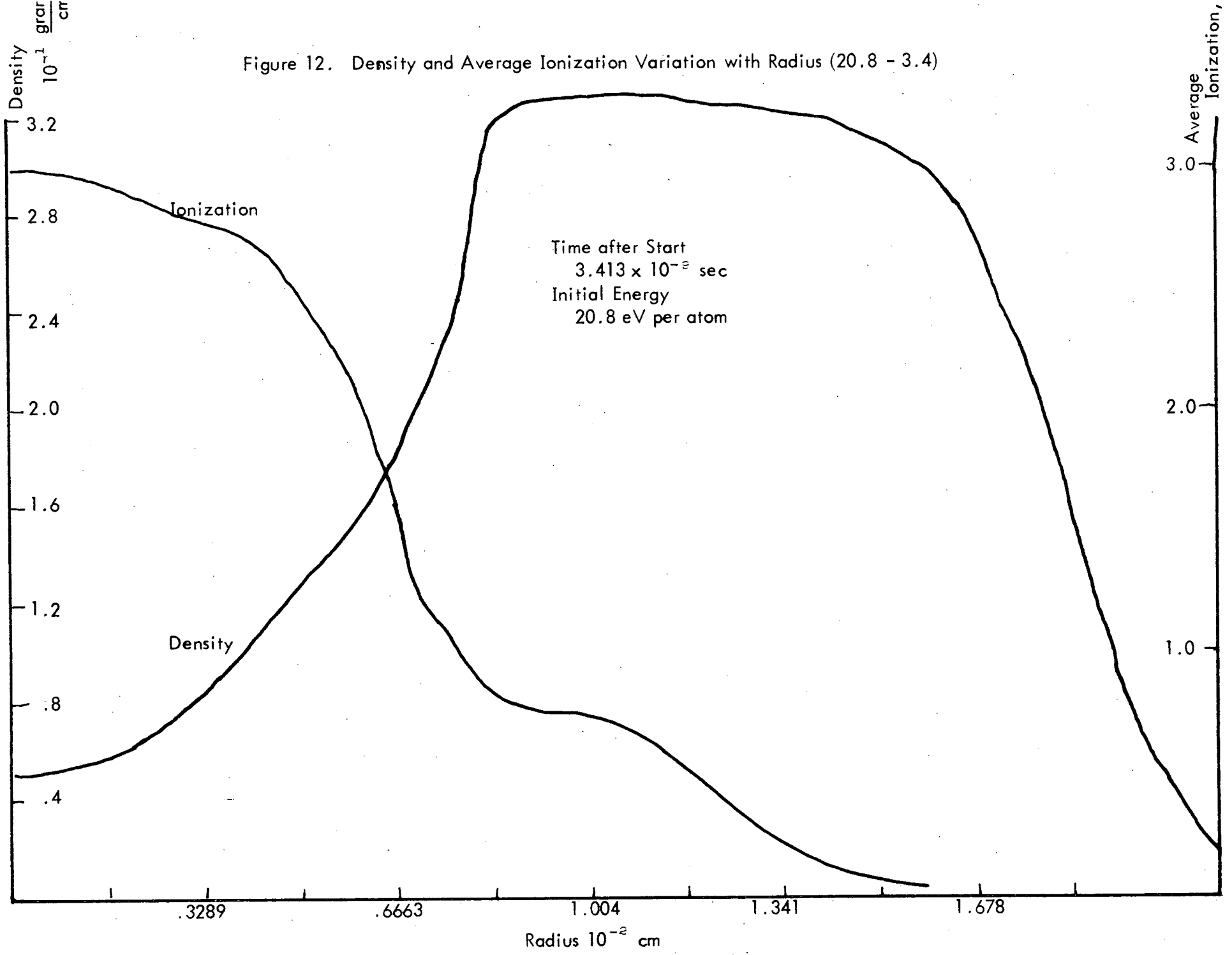

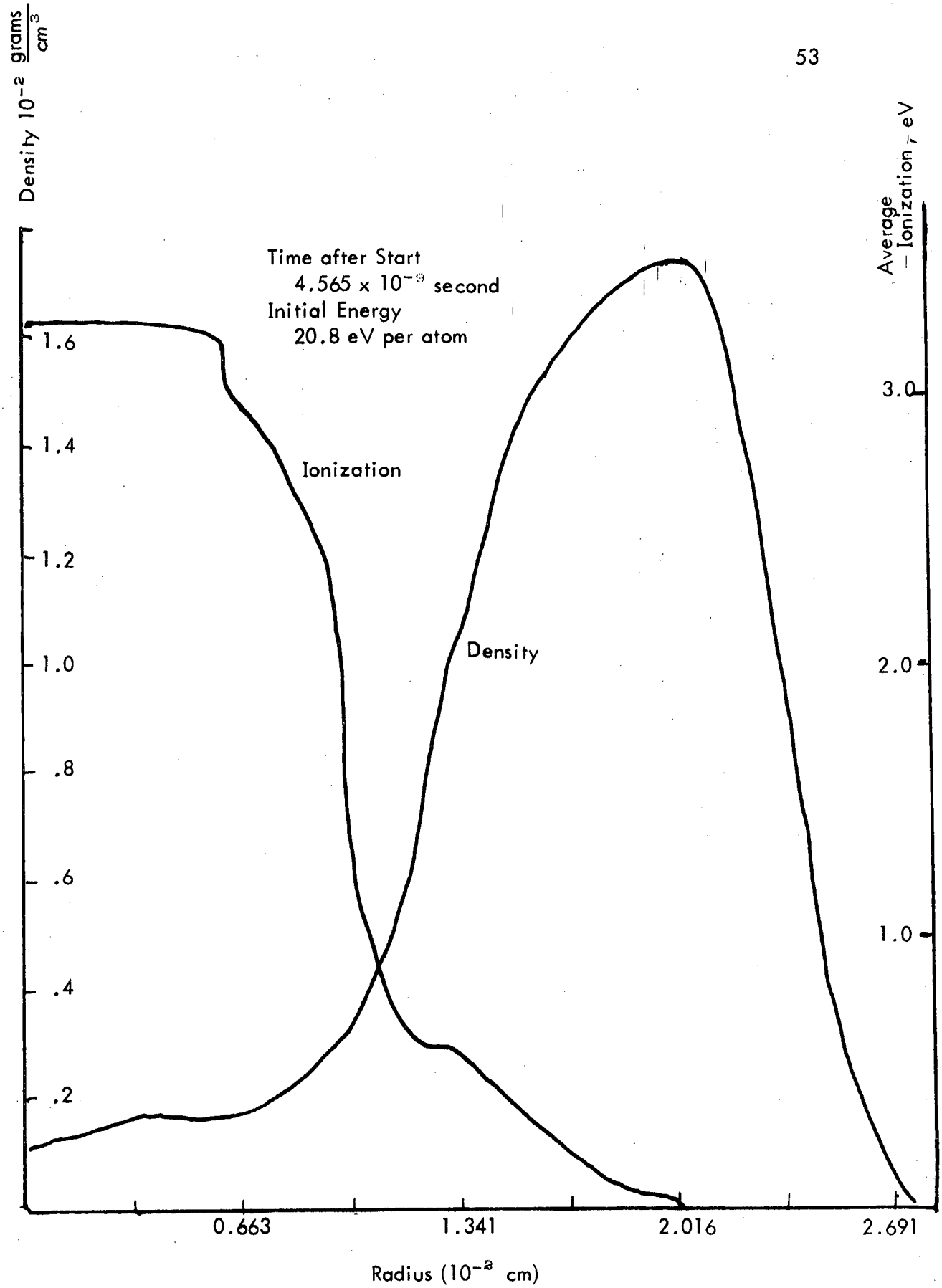

Figure 13. Density and Average Ionization Variation with Radius (20.8 - 4.5)

evidence from the light emission. These are the experiments that have been reported by Brown.

The last graph for the expansion of the plasma with an initial energy of 20.8 eV per atom is designated as Figure 14. This graph shows the expansion at 9.808×10^{-9} seconds after the start of the expansion. An observation of the graphs indicate that the expansion has been computed far beyond the limit at which a practical plasma would be expected to become so unstable that it would disintegrate. The average ionization curve has become rather smooth but it still shows evidence of the 3.0 eV and the 1.0 eV ionization and/or excitation levels.

In comparing the graphs for an initial energy of 20.8 eV per atom with the preceding graphs for an initial energy of 44.45 eV per atom, it is difficult to select the most important factor on which to concentrate. A very interesting subject appears to be the approximate mean radius of the expanding sphere when the density in the core has just dropped into the range from 0.1 to 0.2×10^{-2} grams per cm^3. For the higher initial energy, this radius is in the range between Figure 7 and Figure 8. The subjectively chosen value is 0.0027 cm. In a similarly unreliable manner, the radius is chosen just later than the instant that is represented in Figure 13. Then for the initial energy of 20.8 eV per atom, the value of the radius is taken to be 0.00202 centimeters. Without reference to the time that is required to expand to these limits, it is observed that roughly similar conditions exist between the hot core and the cold shell at the time that these radii were selected. These values are selected while the curves are in close proximity to this discussion in order that they may be easily inspected. There will be a discussion of these measurements after the next set of graphs is presented.

Expansion of a Plasma with an Initial Energy of 7.136 eV per Atom

In order to acquire more information on the effect of the total initial energy on the expansion of a sphere of plasma, some curves are shown for the case when the total initial energy is 7.136 eV per atom. This energy is less than 1/6 of the total energy for the case when the initial energy was 44.45 eV per atom.

With this lower energy, the most important question is to determine if the cold shell still forms around a hot core and the approximate time that is required for this shell to become roughly formed. The curves in Figure 15 represent the state of formation at 4.636×10^{-9}

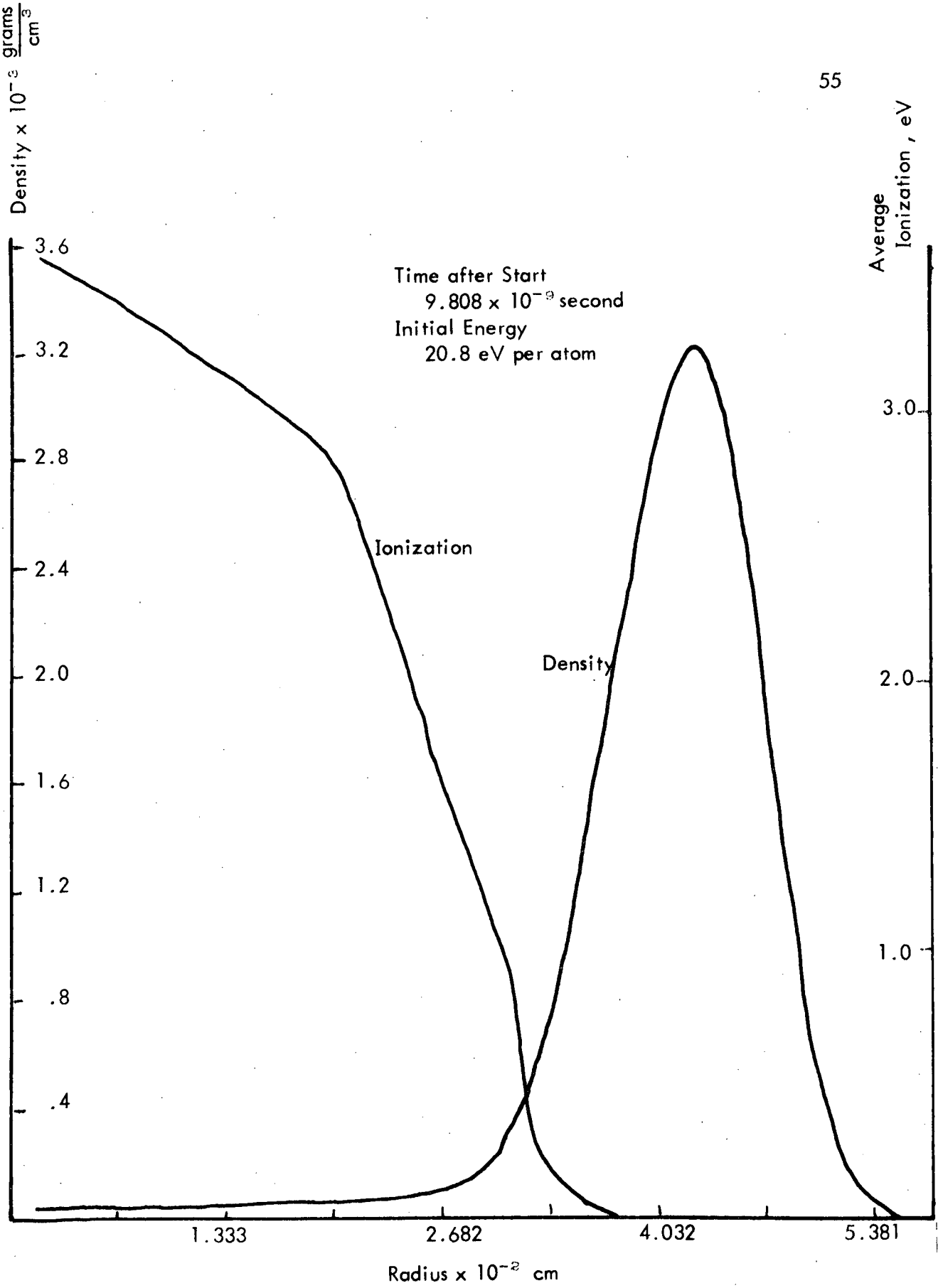

Figure 14. Density and Average Ionization Variation with Radius (20.8 - 9.8)

seconds after the start of the expansion when the initial energy was 7.136 eV per atom. At this time, the hot core is starting to form and the dense, cold shell is beginning to narrow into a peak. The density, as reported by the scale of the ordinate, is down by a factor of about 20 from the initial density.

As the expansion continues, the curves in Figure 16 show the expansion at 7.059×10^{-9} seconds after the start of the expansion. The initial energy of the plasma was 7.136 eV per atom. The curve for the average ionization clarifies some of the up and down variation in the position of the ionization and/or excitation levels near 1.0 eV. In other curves, the level sometimes appeared to be above 1 eV and sometimes below that level. Actually, there are three levels. One is near 1.3 eV, a minor level is near 0.9 eV and a very strong level is at 0.6 eV. The peak of the density in the cold shell is desired for the same purpose.

DISCUSSION OF THE SIGNIFICANCE OF RESULTS FROM THE EXPANSION OF PLASMAS

Some superficial results are repeated to start this discussion. These superficial results were collected at the end of the presentation of the curves on the expansion of the plasma with an initial energy of 44.45 eV per atom.

a. The expansion forms a hot core that is surrounded by a cold shell.

b. Humps, or breaks, in the curvature of the curves for the average ionization indicate the presence of levels for ionization and/or excitation in the plasma. This information was given to the computer by the term that is designated as E_{EXC} in the corrections to the perfect gas law. These levels are not fixed but may appear to be raised, or lowered by the effect of other terms in the equation of state.

c. The curve for the temperature in Figure 9 shows that the so-called cold shell is really cold. In this figure, the temperature falls over three decades within a radial distance that is less than the width of the cold shell.

After the preceding list of specific comments, there are two general subjects which require some discussion. The first subject deals with the formation of the cold shell. It involves the means by which the high temperature and energy in the initial sphere is converted to a high radial velocity. After the comments on the cold shell, the second problem

Figure 15. Density and Average Ionization Variation with Radius (7.13 - 4.9)

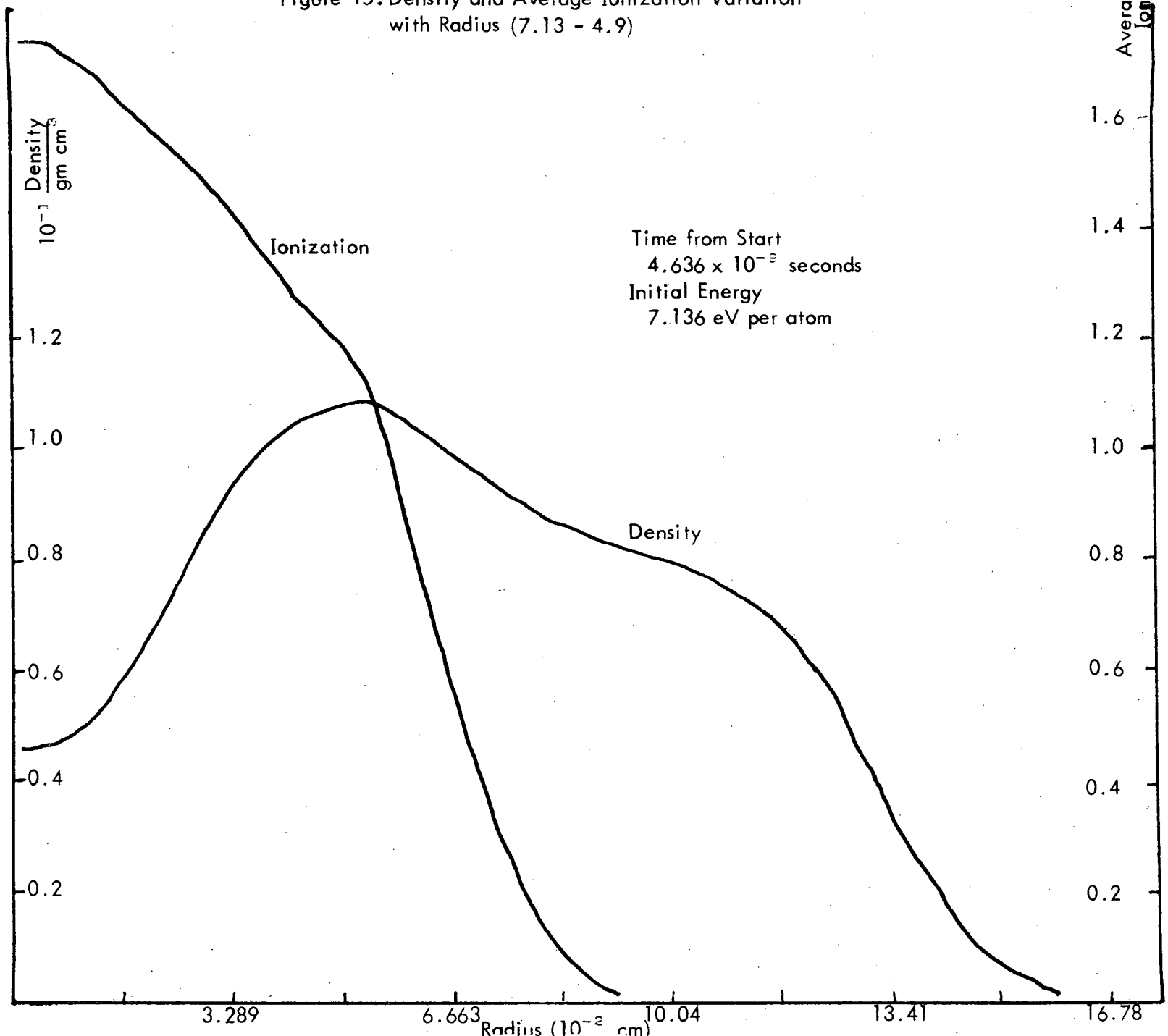

Figure 16. Density and Average Ionization Variation with Radius (7.13 - 7.0)

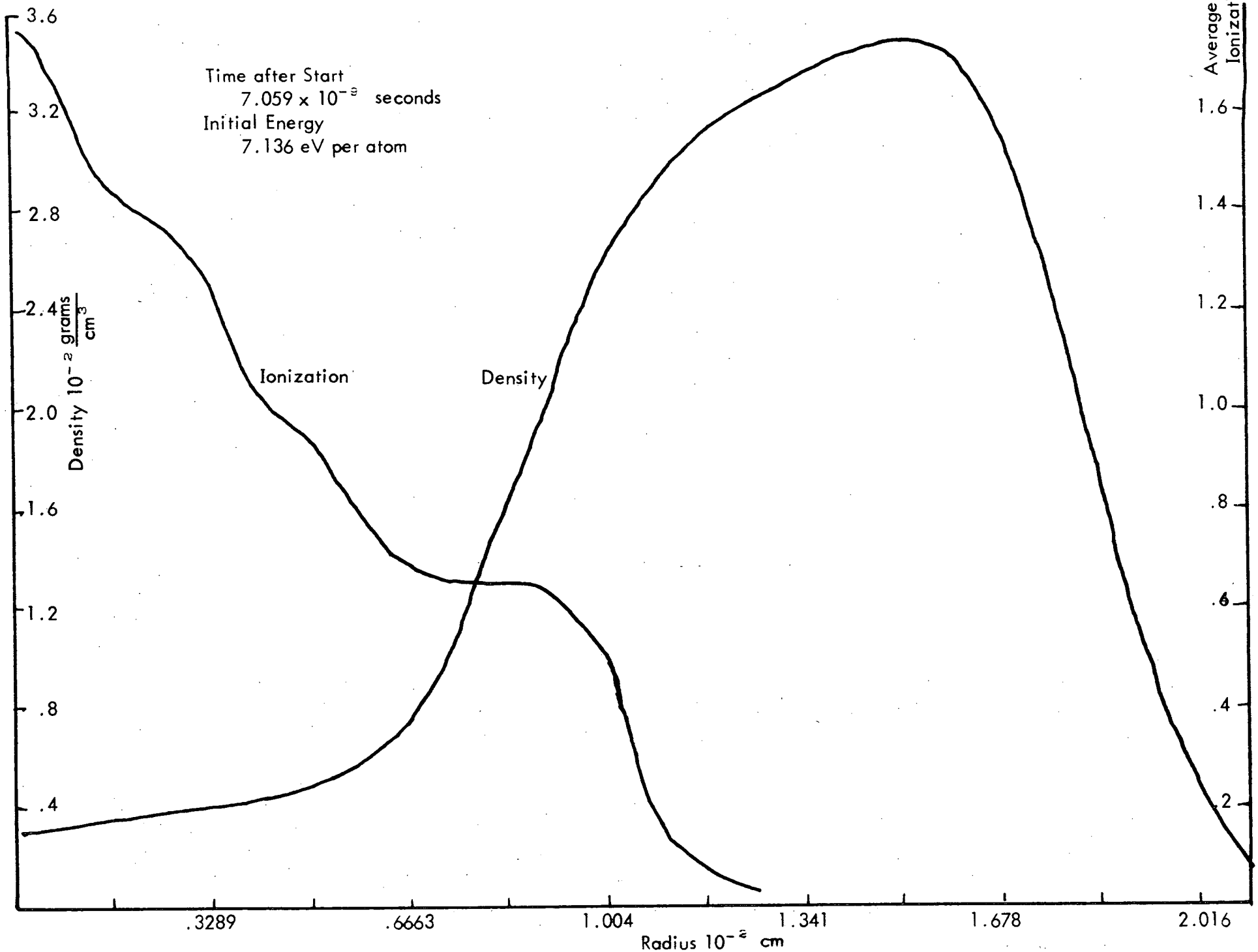

for discussion is the probable evidence that the hot core is squeezed and slowed in expanding.

In the consideration of the first subject on the conversion of temperature to kinetic energy, the following facts are emphasized. There is no energy added to, or subtracted from the sphere during its "free" expansion into a vacuum. There is only a change in the nature of the energy storage. Although the expansion into the vacuum is "free", there is a change in entropy as E_{IN} decreases to zero with the expansion. It is to be recalled that E_{IN} is the energy in the microfields as calculated by cluster integrals. At the start of the expansion, all of the sinks of energy, which are indicated in the equation of state, are filled and the values are placed in the computer which is run until the distribution converges on the correct values. In this way, the energy distribution is in equilibrium. When expansion is allowed to start, the ions and electrons on the outside of the sphere start to move outward from the sphere, but only a small part go out radially. As time progresses, the motion of the outermost ions and electrons become more and more directed outward along radial lines. At the start of the expansion, all of the kinetic energy is randomly directed. With randomly directed velocities, the temperature is given by the relation.

$$\frac{1}{2} m_e \overline{v}^2 = \frac{1}{2} M_{Ion} \overline{V}^2 = \frac{3}{2} k T$$

where m_e is the mass of an electron, and $\overline{v}^2$ is the mean square velocity. M_{Ion} and $\overline{V}^2$ are the same values for the ions and k is the Boltzmann constant.

By the formulation of the equation of state, the radially directed components of the plasma flow is no longer recorded as a temperature. The temperature is composed only of the randomly directed velocities. As an example, the rate of expansion approaches a constant as the sphere grows larger. This constant velocity is obtained when all of the energy in the surface atoms is directed radially outward. As a consequence of the disappearance of the random velocities, the temperature falls to very low values as is apparent by the curve for the temperature in Figure 9.

The second subject for consideration is the relative rates of expansion in the early stages while the hot core is being formed. The radius of the expanding sphere was estimated for the time that the hot core and cold shell were just barely formed. At the end

of the presentation of the graphs for an initial energy of 20.8 eV, there is a collection of subjective data. This collection of data is to show the radius of the peak of the dense, cold shell at a particular instant in the expansion. It is the instant at which the hot core and cold shell are just developed and the lowest density of the hot core has just reached the range between 0.1 and 0.2×10^{-2} grams per cm^3. For an initial energy of 7.136 eV per atom, the radius is taken to be 1.7×10^{-2} centimeters. This data on radii is fragmentary and very subjective. There has been hesitation to add it to this report. The data is presented in Table III.

TABLE III

Subjective Data Illustrating Self-Pressure of Hot Core

Initial Energy	$\sqrt{\text{Initial Energy}}$	$\sqrt{\frac{\text{Initial Energy}}{2.67}}$ Ratio	r cm $\times 10^{-2}$	Predicted r r x Ratio
44.45	6.66	2.50	2.7	6.75
20.8	4.56	1.71	2.02	3.45
7.136	2.67	1.	1.7	1.7

In Table III, the columns have the following significance. The first column is obvious. The second column is the square root of the first column which means that the terms in this column are roughly proportional to the velocity of the final rate of expansion. The third column ranks the relative rates of expansion. They are ranked relative to each other by means of the lowest energy term; i.e. relative to an initial energy of 7.136 eV per atom. The fourth column gives the subjectively selected radii with no consideration of the instant of time after the start of the expansion at which the radius was attained. The fifth column is the product of the subjectively selected value of r by a quantity that is proportional to the final rate of expansion.

The values in the right hand column are the radii that would be expected if no self-pressure was exerted on the hot core by the lowering of the ionization potential and by the energy in the term E_{IN}, etc. This data is interesting but it is certainly not conclusive. In trying to interpret these results, it should be considered that the velocity of

expansion starts slowly and increases with time to the predicted final rate.

There are two more subjects which should be mentioned briefly. The average ionization at the center of the sphere is always higher in the last, or the last few graphs, than the average ionization at the start of the expansion. This is rather surprising in consideration of the lower density and the corresponding lower pressure. No further discussion of this subject is given in this report. There is another interesting fact. The pressure falls very precipitously just inside the cold shell. This pressure is not a proper scaler pressure. It is evidence that a tensor should represent the pressure.

PHASE THREE

ADAPTATION OF A COMPUTER PROGRAM TO A SOLUTION FOR METEOROID BUMPER PENETRATION

INTRODUCTION

The objective of this study is to develop a reliable computer program for the penetration of a thin plate of aluminum by a sphere of quartz. The thin plate of aluminum simulates a bumper plate for micrometeoroids. A good equation of state is available for quartz as well as for aluminum. As the aluminum equation of state was derived, the equation for quartz is based on an experimentally determined Hugoniot curve. Then an equation of state of the Mie-Grunesen type was derived. In addition, an adjustment in the computer program permits the quartz to have any desired porosity.

At the start of this study, a computer program was available for the formation of a crater by the impact of a porous sphere of rock at hypervelocity onto a thick slab of aluminum. Mathematically, the thick slab is a semi-infinite slab of aluminum. The available computer program was formulated by Dr. B. A. Hardage, who is an ex-member of this group. Dr. Hardage is presently a member of the Geophysical Group for Phillips Petroleum Company. Hardage employed this program with considerable success to determine the size and shape of craters that were formed by hypervelocity impact. As will be indicated, it was suitable for that purpose, but simplifying assumptions by Hardage were not appropriate for the penetration of a thin plate of aluminum. With his program, incorrect results were found for the penetration of a thin plate.

The modifications to Hardage's program are being made entirely by Mr. Mark J. Hooker. The modifications have proved to be much more extensive than was anticipated. As a consequence, the final computer program is considered to be developing Mr. Hooker's capabilities far beyond those of the average student who writes a thesis as part of the requirements for an M.S. degree. Since this is Hooker's first major computer program, he has had considerable assistance beyond that which is received by the usual student. Dr. R. E. Bruce helped in changing the differencing method. Dr. Hardage has given

major assistance in emphasizing the limitations of his program, disclosing the exact nature of some assumptions that were not clear, and approving some of the modifications.

The following discussion presents the basis for the changes in the computer program and comments on the results from these changes. Since the modifications vary so widely in importance and in the difficulty of the actual change, they will not be listed separately in this introduction. The changes will be grouped under headings which will indicate the basis for some of the corrections.

TECHNIQUE TO DETERMINE MOMENTUM AT BOTTOM SURFACE OF THIN PLATE

For general information and to assist in formulating the remainder of the problem, it is desired to be able to determine the momentum that reaches the bottom of the thin plate. The only part of immediate interest is from the initial shock when the sphere of rock is incident on the thin plate. The method of obtaining this information is described to assist in interpreting the graphs. It has not been changed for it serves another purpose, it decreases the cost of trouble shooting other changes in the overall program. This last use is discussed before the momentum is considered.

In the curves that have been presented and in the one curve that is given in this report, no tension force is assumed to be exerted between the curvilinear cubes with which the computer deals. Compression was always and still is in the computer program. This is a hold-over from the Hardage program. His program dealt only with compression in the formation of a crater. The spray that "flew up " from the impact zone was released if the internal energy exceeded the energy to melt aluminum. These instructions have not been changed up to the present time. In the portion of the problem in which tension predominates, it permits the plate to disintegrate. There have been so many problems in the compression portion of the problem that this characteristic has been an aid. One advantage of this omission of rupture forces between the curvilinear cubes is the considerable reduction in computer time and in computer printout while correcting other features in the computer program.

A second, more important advantage is that this technique, with proper safeguards, may be employed to estimate the momentum that is involved in the reflection

of the initial shock from the back face which is the bottom face of the thin plate. This may be illustrated by reference to the graph in Figure 17. On the bottom side of the thin plate, there is a hemispherical gap of missing material between columns 10 and 14, counted from right to left. Recall that the initial bottom face was horizontal. This region shows a part of the effect of the incident momentum of the sphere of rock. When the rock reaches the plate, a shock starts from the initial region of contact between the sphere and the plate. The portion of this shock front, which enters the plate, reaches the rear face and "snaps off" a chunk of aluminum as it is reflected from the rear face. The missing material is the mass which is compressed as the initial shock passes it on the path to the back face. This shock compression gives the material that energy which is required to exceed the energy to melt the material. The velocity of departure of this rock may be measured by observation of the graphs from cycles which precede the cycle that is presented in Figure 17. With the mass and the velocity known, the momentum is determined. This is an application of a simple, familiar experiment in physics. Suspend ten balls in a line and in contact. Lift one ball and let it impact on the second ball. Only the tenth ball, at the end of the line, flies up.

ENERGY FOR HYPERVELOCITY SEPARATION OF FRAGMENTS OF THIN ALUMINUM PLATE

In the preceding section, the force to rupture the aluminum was mentioned. It was also indicated that no value for the strength of aluminum had been inserted in the program up to this time. The computer program must always consider that the break occurs over the surface of a curvilinear cube. The failure may be rupture in tension, or it may be a failure in shear. There is some evidence in small regions that the failure may approximate to a plane; however, the most of the ruptures are very rough. This appears to eliminate shear as a major factor. From the observations, most of the ruptures appear to be in failures in tension. The strength in tension for rapid breaks is difficult to obtain, or recognize among the available data. The computer calculation for the graph in Figure 17 was based on the assumption of an impact at 7.2 kilometers per second.

For practical purposes, a simple assumption will be made in order to obtain a good

Figure 17. A Typical Graph of the Performance of the Computer Program for the Impact of a Sphere of Rock (Quartz) on a Thin Plate of Aluminum. The figure represents the situation after about 200 cycles on the computer. Hold the graph with the narrowest squares at the top. The right hand side of the graph represents the position of the diameter of the sphere at the start of the impact. The sphere moves from the top toward the bottom of the graph. At the start of the impact, the hemisphere extends from 1 to 20 with a radius of 10 spaces in the vertical direction. The type and the amount of the information is indicated by the following description of the symbols. Only about half of the information per curvilinear cube is presented. Omitted information includes density, internal energy, kinetic energy, radial momentum, transverse momentum, etc.

In this graph, the symbols are listed below. The symbol in each curvalinear cube.

o	Partly filled with rock, remainder vacuum
O	Completely filled with rock
x	Partly filled with aluminum, remainder vacuum
X	Completely filled with aluminum
II	Partly filled with aluminum, partly filled with rock
III	Partly filled with aluminum, partly filled with rock and partly filled with vacuum

The fractional volume of aluminum and of rock is given in each case.

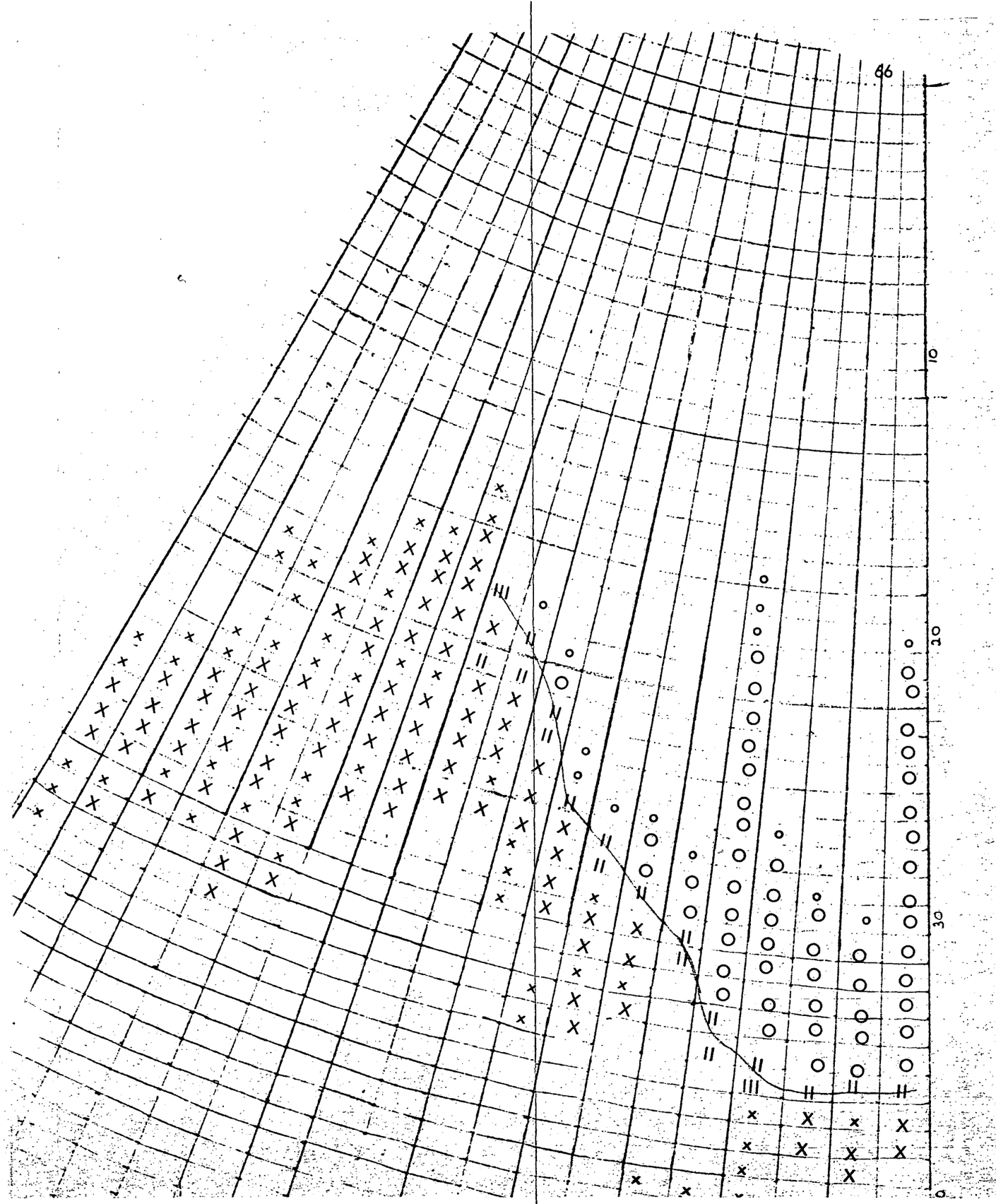

set of values for the final solution. There are two variables to be considered, the rate of separation of the parts and the temperature. High rates of separation will reduce the amount and perhaps even the possibility of ductile failures by the flow of the metal, or liquid. The brittle failures are not of the type which occurs when a crack enters a highly stressed region so the crack constitutes a stress "riser". It is more likely that the pieces will be simply jerked, or knocked apart. Without considering the effect of the rate in more detail, the effect of temperature is considered.

From the internal energy, that is in the print-out from the computer, the temperature of the metal, or liquid will be known. Below the melting point, which is only 659.7°C, the strength of aluminum decreases in a manner that is readily available from references. These values will probably be increased in the final solution provided the effect of the high rate of separation is introduced. For the first, approximate values, the liquid will be required to withstand some force in tension. The exact value will be selected at the last minute. Above the boiling temperature of aluminum at 2057°C, the aluminum is a plasma and will "fly" apart.

APPENDIX A

Typical Substitution of Experimental Results to Evaluate Constants

The evaluation of the constants by employing experimental data illustrates some features of the equation. For this purpose, an evaluation is given below. The general equation, Equation 10, has the following form

$$P_1 s_f = \frac{(P_2)^8}{24} \frac{9P_2 r_o - 7P_3}{(P_3 + P_2 r_o)^9} + \frac{7}{24}\left(\frac{P_2}{P_3}\right)^8$$

The known constants and the known data from one experiment may be inserted to partially evaluate the constants, P_1, P_2 and P_3.

$P_1 = 7.5313 \times 10^9$ D

$s_f = 8$ cm

The dependence of the second constant, P_2 on various values is given by the relation

$P_2 = 4\rho - 3\ell\rho_1$

ℓ is assumed for this evaluation to have the value, 0.01

ρ is the density of aluminum, 2.675

ρ_1 is the average density of the stacked sheets of paper, 0.4609

Then the numerical value of P_2 is given by the relation

$P_2 = 11.060 - 0.01383 = 11.0462$

The dependence of the third constant, P_3, on various values is given by the relation

$P_3 = -6\ell S$

ℓ is assumed for this evaluation to have the value, 0.01

S is taken to be 10 grams per cm^2

Then the numerical value of P_3 is given by the relation

$P_3 = -0.6$

Substitute these constants into the equation at the start of this Appendix.

$$8 \times 7.5313 \times 10^{9} D = \frac{(P_2)^8}{24} \frac{(9 \times 11.0462 \times 0.09525 + 4.2)}{(P_3 + P_2 r_o)^9} + \frac{7}{24}\left(\frac{P_2}{P_3}\right)^8$$

$$6.025 \times 10^{10} D = \frac{(P_2)^8}{(P_3 + P_2 r_o)^9} \frac{13.66935}{24} + \frac{7}{24}\left(\frac{P_2}{P_3}\right)^8$$

Continue with the evaluation by substituting for the remaining values of P_2 and P_3

$$6.025 \times 10^{10} D = \frac{(11.0462)^8}{(-0.6 + 11.0426 \times 0.09525)^9} \frac{13.66935}{24} + \frac{7}{24}\left(\frac{11.0462}{-0.6}\right)^8$$

Two features of this numerical relation should be noted. The first is the critical nature of the denominator in the first term. The denominator is the difference between two relatively small numbers. The difference is positive for this set of values. The other feature to note is that, in the second term, the numerical value inside the bracket is negative. Since this negative value is raised to an even power, 8, the value of the second term is always positive.

$$6.025 \times 10^{10} D = \frac{(11.0462)^8}{(-0.6 + 1.05215)^9} \frac{13.66535}{24} + \frac{7}{24}\left(\frac{11.0462}{-0.6}\right)^8$$

Continue the simplification of this relation

$$6.025 \times 10^{10} D = \frac{(11.0462)^8}{(0.45215)^9} \frac{13.66535}{24} + \frac{7}{24}\left(\frac{11.0462}{0.6}\right)^8$$

After a few arithmetical steps, the equation reduces to

$$D = 2.716$$